BSR/ASHRAE Standard 41.2P

Public Review Draft

Standard Methods for Air Velocity and Airflow Measurement

First Public Review (November 2015)
(Draft Shows Complete Proposed New Standard)

This draft has been recommended for public review by the responsible project committee. To submit a comment on this proposed standard, go to the ASHRAE website at www.ashrae.org/standards-research--technology/public-review-drafts and access the online comment database. The draft is subject to modification until it is approved for publication by the Board of Directors and ANSI. Until this time, the current edition of the standard (as modified by any published addenda on the ASHRAE website) remains in effect. The current edition of any standard may be purchased from the ASHRAE Online Store at www.ashrae.org/bookstore or by calling 404-636-8400 or 1-800-727-4723 (for orders in the U.S. or Canada).

ASHRAE, 1791 Tullie Circle, NE, Atlanta GA 30329-2305

TABLE OF CONTENTS

(This foreword is not part of this standard. It is merely informative and does not contain requirements necessary for conformance to the standard. It has not been processed according to the ANSI requirements for a standard and may contain material that has not been subject to public review or a consensus process. Unresolved objectors on informative material are not offered the right to appeal at ASHRAE or ANSI.))

FOREWORD

Compared to the published version of 41.2 that was reaffirmed in 1992, this revision incorporates air velocity measurements in addition to airflow measurements, and the scope of this standard has been broadened to include field test measurements in addition to laboratory measurements. New sections have been added regarding the test requirements, measurement uncertainty calculations, and test report. Several airflow measurement methods have been included in addition to those found in the previous version. Nozzle airflow measurement test requirements and calculations have been updated. Additionally, this revision meets ASHRAE's mandatory language requirements. Users of this standard who are seeking to measure fan airflow rates should also be aware of ASHRAE Standard 51/AMCA 210 that is used for determining a fan's aerodynamic performance in terms of airflow rate, pressure developed, power consumption, air density, speed of rotation, and efficiency.

1. PURPOSE

This standard prescribes methods for air velocity and airflow measurement, including consideration of density effects.

2. SCOPE

This standard applies to air velocity and airflow measurement for testing heating, ventilating, air conditioning, and refrigerating systems and components at pressures within this range: -25 kPa to +25 kPa (-100 in. of water to +100 in. of water) referenced to atmospheric pressure.

3. Terminology

3.1 Definitions

***accuracy*:** the degree of conformity of an indicated value to a *true value*.

error: the difference between the test result and its corresponding *true value*.

geometrically equivalent diameter: the diameter of a round duct having the same area as a duct that is not round.

hydraulic diameter, D_h: four times the airflow area divided by the perimeter of the solid boundary in contact with the airflow.

mean, $\overline{X}_m$: the arithmetic average of *N* readings.

measurement system: the instruments, signal conditioning systems, and data acquisition system.

sample size: the number of individual values in a sample.

test chamber: an airflow-measuring apparatus that has a chamber diameter that is greater than twice the *unit under test* (UUT) duct diameter or *geometrically equivalent diameter*.

test duct: an airflow-measuring apparatus that has a constant diameter throughout its length except for transition portions at one or both ends.

test point: a specific set of test conditions and tolerances for recording data.

true value: unknown, error-free value of a test result.

uncertainty: a measure of the potential error in a measurement or experimental result that reflects the lack of confidence in the result to a specified level.

unit under test (UUT): equipment that is the subject of liquid flow measurements.

3.2 Symbols

Table 3.1: Symbols Used in this Standard

Symbol	Description	Units (SI)	Units (I-P)
A_x	Area of cross section at plane *x*	m^2	ft^2
C	Nozzle discharge coefficient	Dimensionless	
C_p	Constant pressure specific heat	J/(kg·K)	Btu/(lb_m· °F)
C_v	Constant volume specific heat	J/(kg·K)	Btu/(lb_m· °F)
D_E	Geometrically equivalent diameter	m	ft
D_h	Hydraulic diameter	m	ft
d	Nozzle throat diameter	m	ft
d_f	Fringe spacing	m	ft
d_L	Largest nozzle throat diameter in a multiple nozzle chamber	m	ft
D_{Ex}	Diameter or geometrically equivalent diameter at plane *x*	m	ft
f	Coefficient of friction	Dimensionless	
f_D	Doppler burst frequency	1/s	Hz
h_e	Enthalpy of condensate	kJ/kg	Btu/lb_m
h_s	Enthalpy of steam	kJ/kg	Btu/lb_m
$L_{x,x'}$	Length of duct between planes *x* and *x*'	m	ft
K	Calibration coefficient provided by the instrument manufacturer	Dimensionless	
$\dot{m}$	Mass airflow rate	kg/s	lb_m/h
$\bar{\dot{m}}$	Time-averaged airflow rate	Kg/s	Lb_m/h
N	Number of traverse measurement points	Dimensionless	
n	Number of readings	Dimensionless	
P_s	UUT static pressure	Pa	in. H_2O
P_{sa}	Average static pressure	Pa	in. H_2O
P_{sx}	Static pressure at plane *x*	Pa	in. H_2O
P_t	UUT total pressure	Pa	in. H_2O

P_{ta}	Average total pressure	Pa	in. H_2O
P_{tx}	Total pressure at plane *x*	Pa	in. H_2O
P_v	UUT velocity pressure	Pa	in. H_2O
P_{vx}	Velocity pressure at plane *x*	Pa	in. H_2O
P_b	Corrected barometric pressure	kPa	in. H_2O
P_e	Saturated vapor pressure at t'_x	kPa	in. H_2O
P_p	Partial vapor pressure at plane *x*	kPa	in. H_2O
q	Rate of heat transfer	W	Btu/h
Q	UUT airflow	m^3/s	cfm
Q_{xa}	Average airflow at plane *x*	m^3/s	cfm
$\bar{Q}$	Time-averaged airflow	m^3/s	cfm
Q_x	Airflow at plane *x*	m^3/s	cfm
R	Gas constant	J/(kg·K)	(ft·lb)/(lb_m·R)
Re	Reynolds number	Dimensionless	
t_e	Temperature of condensate	°C	°F
t_x	Dry-bulb temperature	°C	°F
t'_x	Wet-bulb temperature	°C	°F
t_w	Temperature of hot water	°C	°F
T	Time	s	min
v'_x	Specific volume of air at plane x	m^3/kg	ft^3/lb_m
V_{ax}	Average velocity at plane *x*	m/s	fpm
$\bar{V}$	Time-Averaged Velocity	m/s	fpm
V_x	Velocity at plane x	m/s	fpm
W_e	Rate of condensate	kg//h	lb_m/h
W_x	Humidity ratio of air at plane x	kg_{wv}/kg_{da}	lb_{mwv}/lb_{mda}
W_w	Rate of hot water flow	kg/h	lb_m/h
W	Input to heaters	W	Btu/h
y	Thickness of straightener elements	m	ft
β	Ratio of nozzle throat diameter to duct diameter	Dimensionless	
ε	Compressibility Factor	Dimensionless	
γ	Ratio of specific heats	Dimensionless	
$\Delta p_{x,x'}$	Pressure differential between planes *x* and x'	Pa	in. H_2O
κ	Half-angle between laser beams	deg	rad
λ	Laser wavelength	m	ft
μ	Air viscosity	$(N·s)/m^2$	lb_m/(ft·s)

ρ_x	Air density at plane *x*	kg/m^3	lb$_m$/ft^3
$\sum$	Summation sign	Dimensionless	

3.3 Subscripts

Table 3.2: Subscripts

Subscript	Description
r	Readings
target	Target Velocity or Mass Flowrate
i	Index Subscript
x	Plane 0, 1, 2, 3, 4, 5, 6, 7, or 8
0	Plane 0 (ambient test area)
1	Plane 1 (entering UUT)
2	Plane 2 (leaving UUT)
3	Plane 3 (entering Pitot-static traverse)
4	Plane 4 (entering duct piezometer)
5	Plane 5 (entering nozzle(s))
6	Plane 6 (leaving nozzle(s))
7	Plane 7 (entering test apparatus)
8	Plane 8 (leaving test apparatus)

4. CLASSIFICATIONS

4.1 Air Velocity and Airflow Measurement Applications. Air velocity and airflow measurement applications that are within the scope of this standard are classified as one of the following two types.

4.1.1 Laboratory Applications. Air velocity and airflow measurements under laboratory conditions are engineering development tests or tests to determine product ratings. **(Informative Note):** Laboratory air velocity and airflow measurements tend to use more accurate instruments than field measurements and tend to meet the instrument manufacturer's installation requirements.

4.1.2 Field Applications. Air velocity and airflow measurements under field conditions are tests to determine ventilation rates or installed system air velocities and airflows. **(Informative Note):** Field air velocity and airflow measurements tend to use less accurate instruments than laboratory measurements and often do not meet the instrument manufacturer's installation requirements.

4.2 Airflow Meter Categories

4.2.1 Mass Airflow Meters. Airflow meters in this category perform direct measurement of air mass flow rates.

4.2.2 Volumetric Airflow Meters. Airflow meters in this category perform direct measurement of volumetric airflows. If air mass flow rates are required, each volumetric airflow measurement shall be multiplied by the air density at the flow measurement location to obtain the air mass flow rate measurement.

4.3 Air Velocity Measurement Methods. Methods of air velocity measurement methods that are within the scope of this standard are the methods listed below. These measurement methods are described in Section 7. **(Informative Note):** Any measured average airflow velocity can be multiplied by the area of the duct in the measurement plane to obtain a volumetric airflow rate.

a. Pitot-static Tube
b. Thermal Anemometer
c. Rotating Vane Anemometer
d. Ultrasonic Velocity
e. Drag-Force Velocity
f. Laser Doppler Velocimeter

4.4 Airflow Measurement Methods. Methods of airflow measurement that are within the scope of this standard are the methods listed below. These measurement methods are described in Section 9.

a. Pitot-static Tube
b. Single and Multiple Nozzle Chambers
c. Thermal Dispersion Array
d. Vortex-Shedding Array
e. Turbine Flowmeter
f. Capture Hoods
g. Tracer Gas

4.5 Standard Air Density. For the purposes of this standard, standard air density = 1.202 kg/m^3 (exact), (0.075 lb_m/ft^3). The conversion uncertainty associated with calculating air velocity or airflow measurement uncertainties in I-P units is ±0.00004 lb_m/ft^3. **(Informative Note):** Annex D provides the derivation of this conversion uncertainty and a description of how this conversion uncertainty is applied to airflow measurement uncertainty calculations.

4.6 Test Apparatus. A test apparatus used to measure air velocity or airflow that includes instruments, airflow-conditioning elements, and airflow-control elements within a sealed conduit. These are classified as *test ducts* or *test chambers* as defined in Sections 4.6.1 or 4.6.2, respectfully.

4.6.1 Test Duct. A *test duct* is a test apparatus that has a constant *geometrically equivalent diameter* throughout its length except for transition portions at one or both ends.

4.6.2 Test Chamber. A *test chamber* is a test apparatus that has a diameter or geometrically equivalent diameter that is greater than twice the UUT duct *geometrically equivalent diameter*.

5. REQUIREMENTS

5.1 Test Plan. A test plan is required. The test plan shall specify the test points and the required measurement system accuracy at each test point. A test plan is a document or other form of communication that specifies the tests to be performed and the required measurement accuracy for each test. Sources of the test plan are (a) the person or the organization that authorized the tests to be performed, (b) a method of test standard, (c) a rating standard, or (d) a regulation or code.

5.2 Values to be Determined and Recorded

5.2.1 Values to be Determined and Recorded for Air Velocity Measurements

5.2.1.1 Air velocity if required by the test plan in Section 5.1, m/s (ft/s)

5.2.1.2 The uncertainty in each air velocity measurement shall be estimated as described in Section 10 for each data point or the worst-case uncertainty for all data points shall be estimated and reported for each data point.

5.2.2 Values to be Determined and Recorded for Airflow Measurements

5.2.2.1 Standard volumetric airflow if required by the test plan in Section 5.1, standard m^3/s at 1.202 kg/m^3, (scfm at 0.075 lb_m/ft^3)

5.2.2.2 Volumetric airflow at the measured density if required by the test plan in Section 5.1, m^3/s (cfm)

5.2.2.3 Mass rate of airflow if required by the test plan in Section 5.1, kg/s (lb_m/h)

5.2.2.4 The uncertainty in each airflow measurement shall be estimated as described in Section 10 for each data point or the worst-case uncertainty for all data points shall be estimated and reported for each data point.

5.3 Test Requirements

5.3.1. Air Velocity Measurement Requirements

5.3.1.1 Air Velocity Measurement Accuracy. A selected air velocity measurement method shall meet or exceed the required air velocity measurement system accuracy over the full range of operating conditions specified in the test plan in Section 5.1.

5.3.1.2 Air Velocity Uncertainty. The uncertainty in each air velocity measurement shall be estimated as described in Section 10 for each test point. Alternatively, the worst-case uncertainty for all test points shall be estimated and reported for each test point.

5.3.1.3 Air Velocity Steady-State Tests. If the test plan in Section 5.1 requires air velocity data points to be recorded at steady-state test conditions but does not specify the steady-state criteria, then the criteria in Equation 5.3.1.1 shall be met if the test plans specifies a target air velocity for steady-state test conditions.

$$\left| \frac{\bar{V} - V_{target}}{V_{target}} \right| \leq 1\% \qquad 5.3.1.1$$

where

V_{target} = target air velocity for the steady-state test conditions specified in the test plan, m/s (fpm)

$\bar{V}$ = the mean air velocity obtained from Equation 5.3.1.2, m/s (fpm)

n = number of measurement samples. There shall be at least 10 measurement samples as required by Equation 5.3.1.3.

$$\bar{V} = \frac{1}{n}\sum_{i=1}^{n} V_i, \text{ m/s (fpm)} \qquad 5.3.1.2$$

$$n \geq 10 \qquad 5.3.1.3$$

If the test plan in Section 5.1 requires air velocity data points to be recorded at steady-state test conditions but does not specify the steady-state criteria, and if no specific target air velocity is specified in the test plan, then steady-state conditions shall be established where at least three consecutive measurements of the mean air velocity in accordance with Equation 5.3.1.2 are equal within ±1%.

5.3.1.4 Operating Limits. Operating conditions during air velocity data measurements shall not exceed limits for pressure, pressure differential, temperature, air velocity, or pressure pulsations specified in the test plan in Section 5.1 or by the air velocity meter manufacturer to achieve the measurement system accuracy required by the test plan.

5.3.1.5 Airflow Leakage Requirements. Unless otherwise specified in the test plan in Section 5.1, measured airflow leakage into or out of the test apparatus shall not be greater than the 0.25% of the airflow at the pressure corresponding to the measured airflow specified in the test plan for laboratory measurements and 1% of the airflow at the pressure corresponding to the measured airflow specified in the test plan for field measurements.

5.3.2. Airflow Measurement Requirements

5.3.2.1 Airflow Measurement Accuracy. A selected airflow measurement method shall meet or exceed the required airflow measurement system accuracy over the full range of operating conditions specified in the test plan in Section 5.1.

5.3.2.2 Airflow Uncertainty. The uncertainty in each airflow measurement shall be calculated as described in Section 10 for each test point. Alternatively, the worst-case uncertainty for all test points shall be estimated and reported for each test point.

5.3.2.3 Airflow Steady-State Tests

5.3.2.3.1 Volumetric Airflow Steady-State Tests. If the test plan in Section 5.1 requires volumetric airflow rate data points to be recorded at steady-state test conditions but does not specify the steady-state criteria, then the criteria in Equation 5.3.2.1 shall be met if the test plans specifies a target volumetric airflow rate for steady-state test conditions.

$$\left|\frac{\bar{\dot{Q}}-\dot{Q}_{target}}{\bar{\dot{Q}}}\right| \leq 1.0\% \qquad 5.3.2.1$$

where

Q_{target} = target volumetric airflow rate for steady-state test conditions specified in the test plan, m^3/s (cfm)

$\bar{Q}$ = the mean value of volumetric airflow rate measurements obtained from Equation 5.3.2.2, m^3/s (cfm)

n = number of measurement samples. There shall be at least 10 measurement samples as required by Equation 5.3.2.3.

$$\bar{Q} = \frac{1}{n}\sum_{i=1}^{n} Q_i \text{ , m}^3\text{/s (cfm)} \qquad 5.3.2.2$$

$$n \geq 10 \qquad 5.3.2.3$$

If the test plan requires volumetric airflow data points to be recorded at steady-state test conditions but does not specify the steady-state criteria, and if no specific target volumetric airflow rate is specified in the test plan, the steady-state mass airflow rate conditions shall be established where at least three consecutive measurements of the mean volumetric airflow rate in accordance with Equation 5.3.2.2 are equal within ±1%.

5.3.2.3.2 Mass Airflow Steady-State Tests. If the test plan in Section 5.1 requires mass airflow rate data points to be recorded at steady-state test conditions but does not specify the steady-state criteria, then the criteria in Equation 5.3.2.4 shall be met if the test plans specifies a target mass airflow rate for steady-state test conditions.

$$\left|\frac{\bar{\dot{m}} - \dot{m}_{target}}{\dot{m}}\right| \leq 1.0\% \qquad 5.3.2.4$$

where

$\dot{m}_{target}$= target mass airflow rate for steady-state test conditions specified in the test plan, kg/s (lb_m/h)

$\bar{\dot{m}}$ = the mean value of mass airflow rate measurements obtained from Equation 5.3.2.5, kg/s (lb_m/h)

n = number of measurement samples. There shall be at least 10 measurement samples as required by Equation 5.3.2.6.

$$\bar{\dot{m}} = \frac{1}{n}\sum_{i=1}^{n} \dot{m}_i \text{, kg/s (lb}_m\text{/h)} \qquad 5.3.2.5$$

$$n \geq 10 \qquad 5.3.2.6$$

If the test plan requires mass airflow data points to be recorded at steady-state test conditions but does not specify the steady-state criteria, and if no specific target mass airflow rate is specified in the test plan, the steady-state mass airflow rate conditions shall be established where at least three consecutive measurements in accordance with Equation 5.3.2.5 of the mean mass airflow rate are equal within ±1%.

5.3.2.4 Operating Limits. Operating conditions during airflow data measurements shall not exceed limits for pressure, pressure differential, temperature, air velocity, or pressure pulsations specified in the test plan in Section 5.1 or by the airflow meter manufacturer to achieve the measurement system accuracy required by the test plan.

5.3.2.5 Airflow Leakage Requirements. Unless otherwise specified in the test plan in Section 5.1, measured airflow leakage into or out of the test apparatus shall not be greater than the 0.25% of the airflow at the leak test pressure equal to the maximum operating pressure in the test plan for laboratory measurements, or 1% of the airflow at the leak test pressure equal to the maximum operating pressure in the test plan for field test measurements.

5.4 Thermodynamic Properties of Air

The thermodynamic properties of the dry air and moist air shall be obtained from ASHRAE RP-1485.[1]

6. INSTRUMENTS

6.1 Instrumentation Requirements for All Measurements

6.1.1 Instruments and data acquisition systems shall be selected to meet the measurement system accuracy specified in the test plan in Section 5.1.

6.1.2 Measurements from the instruments shall be traceable to primary or secondary standards calibrated by the National Institute of Standards and Technology (NIST) or to the Bureau International des Poids et Mesures (BIPM) if a National Metrology Institute (NMI) other than NIST is used. In either case, the indicated corrections shall be applied to meet the uncertainty stated in subsequent sections. Instruments shall be recalibrated on regular intervals that do not exceed the intervals prescribed by the instrument manufacturer and calibration records shall be maintained. Instruments shall be installed in accordance with the instrument manufacturer's requirements, or the manufacturer's accuracy does not apply.

6.1.3 Instruments shall be applied and used in compliance with the following standards:

a. Temperature: ASHRAE 41.1[2] if temperature measurements are required.
b. Pressure: ASHRAE 41.3[3] if pressure measurements are required.
c. Humidity: ASHRAE 41.6[4] if humidity measurements are required.
d. Electrical Power or Shaft Power: ASHRAE 41.11[5] if electrical or shaft power measurements are required.

6.2 Temperature Measurements. If temperature measurements are required by test plan in Section 5.1, the measurement system accuracy shall be within the following limits unless otherwise specified in the test plan:

a. Temperature sensors within ±0.28°C (±0.5°F).
b. Temperature difference sensors within ±l% of the temperature difference being measured.

6.3 Pressure Measurements

6.3.1 Laboratory Pressure Measurements

6.3.1.1 If pressure measurements are required by the test plan in Section 5.1, the measurement system accuracy shall be within ±1.0% of reading unless otherwise specified in the test plan. If absolute pressure sensors are not used, the barometric pressure shall be added to obtain absolute pressure values prior to performing uncertainty calculations.

6.3.1.2 If differential pressure measurements are required by the test plan in Section 5.1, the measurement system accuracy shall be within ±1.0% of reading unless otherwise specified in the test plan. Pressure shall be measured in close proximity to the flow meter in compliance with the flow meter manufacturer's specifications.

6.3.2 Field Pressure Measurements

6.3.2.1 If pressure measurements are required by the test plan in Section 5.1, the measurement system accuracy shall be within ±3.0% of reading unless otherwise specified in the test plan.

If absolute pressure sensors are not used, the barometric pressure shall be added to obtain absolute pressure values prior to performing uncertainty calculations.

6.3.2.2 If differential pressure measurements are required by the test plan in Section 5.1, the errors shall be within ±3.0% of reading unless otherwise specified in the test plan. Pressure shall be measured in close proximity to the flow meter in compliance with the flow meter manufacturer's specifications.

6.4 Electrical Power Measurements. If electrical power measurements are required by the test plan in Section 5.1, the measurement system accuracy shall be within ±1.0% of reading.

6.5 Steam-Flow Measurement. If steam-flow rate measurements are required by the test plan in Section 5.1, the measurement system accuracy shall be within ±1.0% of reading.

6.6 Time Measurements. If time measurements are required by the test plan in Section 5.1, the measurement system accuracy shall be within ±0.5% of the elapsed time measured, including any uncertainty associated with starting and stopping the time measurement unless (a) otherwise specified in the test plan, or (b) a different value for the measurement system accuracy in time measurement is required to be consistent with the required air velocity or airflow measurement accuracy.

7. AIR VELOCITY MEASUREMENT METHODS

7.1 Constraint on All Airflow Measurement Methods. A selected airflow measurement plane shall exceed 7.5 geometrically equivalent diameters downstream of an obstruction or any change in the airflow direction and shall exceed 3 geometrically equivalent diameters upstream of an obstruction or change in the airflow direction unless otherwise specified by the airflow measurement instrument manufacturer. For a rectangular duct with interior width and height dimensions equal to *"a"* and *"b"* respectively, the geometrically equivalent diameter shall be obtained from Equation 7.1.1. For a round duct, the geometrically equivalent diameter, D_E, is equal to the interior diameter, *D*.

$$D_E = \sqrt{\frac{4ab}{\pi}} \qquad 7.1.1$$

7.2 Pitot-Static Tube Air Velocity Measurement Methods. The air velocity measurement methods in this section are based upon Pitot-static tube measurement principles.

7.2.1 Single Pitot-Static Tube Air Velocity Measurement. Figure 7.2.1. shows an example of Pitot-static tube construction and the tubing connections to manometers or a differential pressure transducer to obtain both dynamic (velocity) and static pressures that are used to determine air velocities at a single measurement point. Pitot-static tubes shall be aligned within ±10 degrees of the airflow direction, and any misalignment shall be included in the uncertainty estimate. **(Informative Note):** Negative values of the dynamic (or velocity) pressure readings result from misalignment of the probe and are due to the stagnation port pressure being lower than the static port pressure. This is a clear indication that the Pitot-static tube is not properly aligned with the direction of air velocity.

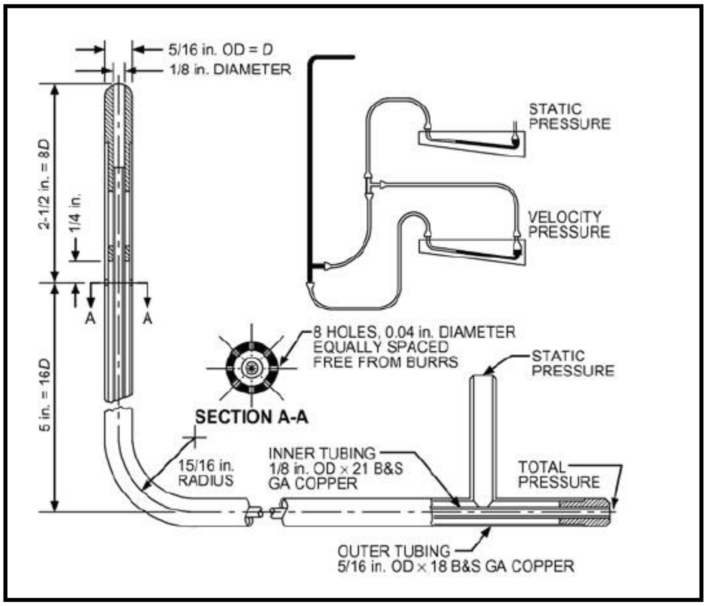

Figure 7.2.1: An Example of Pitot-Static Tube Construction and Connections

7.2.1.1 Velocity Pressure. The total pressure, P_t, is the sum of the static pressure, P_s, and the velocity pressure, P_v, at the measurement location. The velocity pressure shall be obtained from Equation 7.2.1.1.

$$P_v = P_t - P_s \qquad 7.2.1.1$$

7.2.1.2 Air Velocity. The air velocity at the measurement location shall be obtained from Equation 7.2.1.2 in SI units or from Equation 7.2.1.3 in I-P units.

$$V = K\sqrt{\frac{2P_v}{\rho_x}} \qquad 7.2.1.2$$

$$V = 1097.8K\sqrt{\frac{P_v}{\rho_x}} \qquad 7.2.1.3$$

7.2.2 Pitot-Static Tube Traverse Air Velocity Measurement. The process of sequentially positioning a single Pitot-static tube at different measuring points within a measurement plane to measure air velocities is called a Pitot-static tube traverse. Prescribed Pitot-static traverse measuring points within a measurement plane are shown in Figure 7.2.2 for both rectangular and round ducts. Pitot-static tubes shall be aligned within ± 10 degrees of the airflow direction, and any misalignment shall be included in the uncertainty estimate. **(Informative Note 1):** Negative dynamic (or velocity) pressure readings, which indicate that the stagnation port pressure is less than the pressure sensed at the static ports, are a clear indication that the Pitot-static tube is not properly aligned with the direction of air velocity. **(Informative Note 2):** Severe errors are also possible even if negative pressure readings are not observed. It is critical that the flow direction be known and the probe be properly aligned with the flow direction. **(Informative Note 3):** Traversing techniques have also been applied to other velocity measurement methods, including hot-wire and hot-film anemometers.

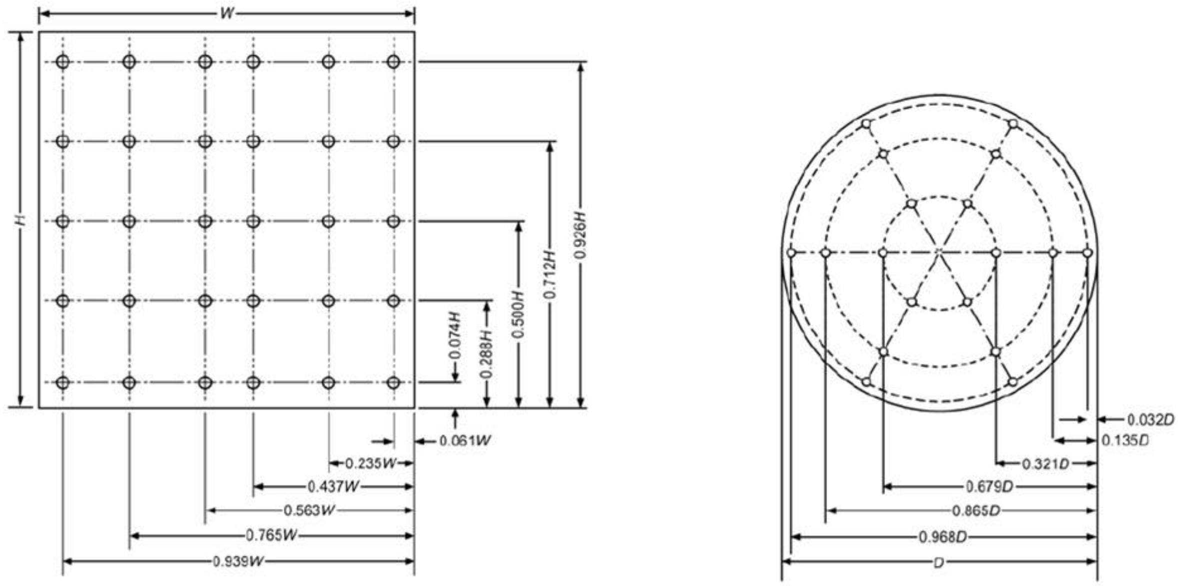

Duct Dimensions	No. of Points for Traverse Lines	Position Relative to Inner Wall
18 in. < H, W < 30 in.	5	0.074, 0.288, 0.500, 0.712, 0.926
30 in. ≤ H, W ≤ 36 in.	6	0.061, 0.235, 0.437, 0.563, 0.765, 0.939
H, W > 36 in.	7	0.053, 0.203, 0.366, 0.500, 0.634, 0.797, 0.947

Log-Tchebycheff Rule for Rectangular Ducts

No. of Measuring Points per Diameter	Position Relative to Inner Wall
6	0.032, 0.135, 0.321, 0.679, 0.865, 0.968
8	0.021, 0.117, 0.184, 0.345, 0.655, 0.816, 0.883, 0.979
10	0.019, 0.077, 0.153, 0.217, 0.361, 0.639, 0.783, 0.847, 0.923, 0.981

Log-Linear Rule for Circular Ducts

Note: Example duct has 5 × 6 (*H* × *W*) measurement pattern, as for rectangular duct of 24 × 30 in.

**Figure 7.2.2. Pitot-Tube Traverse Measuring Points
for Rectangular Ducts and Round Ducts**

7.2.2.1 Velocity Pressure. The total pressure, P_{ti}, is the sum of the static pressure, P_{si}, and the velocity pressure, P_{vi}, at the traverse measurement point. The velocity pressure at each traverse measurement point shall be obtained from Equation 7.2.2.1.

$$P_{vi} = P_{ti} - P_{si} \qquad 7.2.2.1$$

7.2.2.2 Average Velocity Pressure. The average velocity pressure, P_{va}, shall be obtained from Equation 7.2.2.2.

$$P_{va} = \left(\frac{\sum_{i=1}^{N}\sqrt{P_{vi}}}{N}\right)^2 \qquad 7.2.2.2$$

7.2.2.3 Average Air Velocity. The average air velocity shall be obtained from Equation 7.2.2.3 in SI units or from Equation 7.2.2.4 in I-P units.

$$V_a = K\sqrt{\frac{2P_{va}}{\rho_x}} \qquad 7.2.2.3$$

$$V_a = 1097.8K\sqrt{\frac{P_{va}}{\rho_x}} \qquad 7.2.2.4$$

7.2.3 Self-Averaging Array Air Velocity Measurement. Self-averaging arrays consist of multiple bifurcated or extruded tubes spread out over a measurement plane that have holes to sample and self-average both total and static pressure across the measurement plane. The self-averaged total pressure is connected to one side of a differential pressure transducer and the self-averaged static pressure is connected to the other side of the same pressure transducer.

7.2.3.1 Average Velocity Pressure. The average total pressure, velocity pressure, P_{va}, in the measurement plane shall be obtained from Equation 7.2.3.1.

$$P_{va} = P_{ta} - P_{sa} \qquad 7.2.3.1$$

7.2.3.2 Average Air Velocity. The average air velocity shall be obtained from Equation 7.2.3.2 in SI units or from Equation 7.2.3.3 in I-P units.

$$V_a = K\sqrt{\frac{2P_{va}}{\rho_x}} \qquad 7.2.3.2$$

$$V_a = 1097.8K\sqrt{\frac{P_{va}}{\rho_x}} \qquad 7.2.3.3$$

7.2.4 Self-Averaging Probe Air Velocity Measurement. Self-averaging probes include multiple total and static pressure ports along a straight line or around a circumference within the airstream. The self-averaged total pressure is connected to one side of a differential pressure transducer, and the self-averaged static pressure is connected to the other side of the same pressure transducer.

7.2.4.1 Average Velocity Pressure. The average total pressure, velocity pressure, P_{va}, in the measurement plane shall be obtained from Equation 7.2.4.1

$$P_{va} = P_{ta} - P_{sa} \qquad 7.2.4.1$$

7.2.4.2 Average Air Velocity. The average air velocity shall be obtained from Equation 7.2.4.2 in SI units or from Equation 7.2.4.3 in I-P units.

$$V_a = K\sqrt{\frac{2P_{va}}{\rho_x}} \qquad 7.2.4.2$$

$$V_a = 1097.8K\sqrt{\frac{P_{va}}{\rho_x}} \qquad 7.2.4.3$$

7.3 Thermal Anemometer. The thermal anemometer incorporates one of the following velocity sensors at the sensing end of a probe: (a) a heated resistance temperature device, (b) a thermocouple junction, or (c) a thermistor sensor. Air movement past the electrically-heated velocity sensor cools the sensor in proportion to the speed of the airflow. Commercial thermal anemometers include associated equipment to collect and average the individual air velocity measurements to provide the resulting measured average air velocity for display or automated data recording. **(Informative Note 1):** Unlike a Pitot-static probe, which can provide some warning of severe misalignment by giving a negative reading, a thermal anemometer always indicates a positive velocity reading, even if the flow direction is reversed. **(Informative Note 2):** For user information, see Informative Annex E Section E6.

7.4 Rotary Vane Anemometers. Rotary vane anemometers provide a direct readout of air velocity based upon the wheel revolution rate. Rotary vane anemometers shall be aligned with the airflow direction within ±10 degrees, and any misalignment shall be included in the uncertainty estimate.

7.5 Ultrasonic Velocity Meters. Ultrasonic meters measure air velocity. Clamp-on ultrasonic flow meters measure air velocity within a pipe or tube without being inserted into the airflow stream. **(Informative Note 1):** Immersion-type ultrasonic flowmeters are also commercially available. **(Informative Note 2):** For further reading, see Informative Annex A citation A3.

Ultrasonic flowmeters use the transit-time method to measure the effect that flow velocity has on bi-directional acoustical signals. An upstream transducer sends a signal to a downstream transducer that then returns a signal. When air is not flowing, the time for the signal to go from one transducer to another, in either direction, is constant. Air velocity causes the acoustical signal to increase speed in the direction of flow and reduces the acoustical signal speed in the upstream direction. This creates the time difference that correlates to the airflow velocity. **(Informative Note):** For further reading, see Informative Annex A citation A5.

7.6 Drag-Force Velocity Meters. Drag-force flowmeters determine air velocity. Piezoelectric or strain-gage methods are used to sense dynamic drag-force variations. Air velocity shall be obtained from Equation 7.6.1 in SI units, or obtained from Equation 7.6.2 in I-P units. **(Informative Note):** For further reading, see Informative Annex A Section A3**.**

In SI units:

$$V = \sqrt{\frac{2\,f_d}{C_d A \rho_x}} \qquad 7.6.1$$

where

V = calculated air velocity, m/s
f_d = measured drag force, N
C_d = drag coefficient specified by the meter manufacturer, dimensionless
A = cross-section area, m^2
ρ_x = air density at the measurement plane, kg/m^3

In I-P units:

$$V = \sqrt{\frac{2\,g_c f_d}{C_d A \rho_x}} \qquad 7.6.2$$

where

V = calculated air velocity, ft/s
f_d = measured drag force, lb_f
C_d = drag coefficient specified by the meter manufacturer, dimensionless
A = cross-section area, ft^2
ρ_x = air density at measurement plane, lb_m/ft^3
g_c = gravitational constant, 32.174 $(lb_m\text{-ft})/(lb_f\text{-s}^2)$

7.7 Laser Doppler Velocimeter. A Laser Doppler Velocimeter (LDV) is an optical measurement system that collects scattered light produced by particles that are seeded into the airstream that pass through two intersecting laser beams that have the same light frequency as shown in Figure 7.8.1.

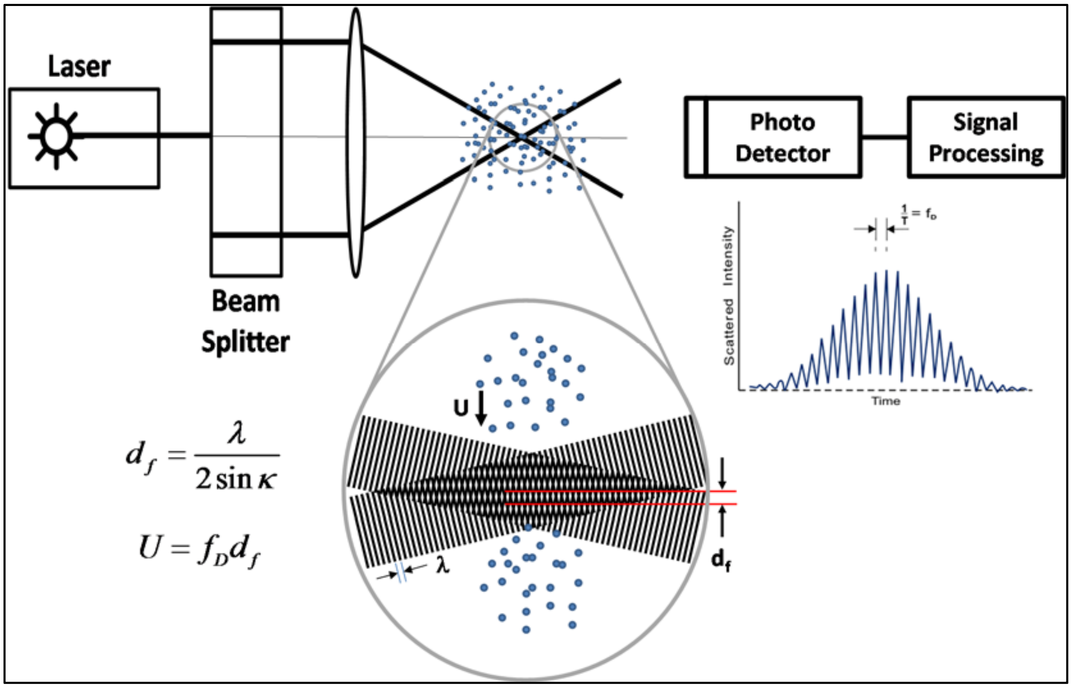

Figure 7.8.1: Laser Doppler Velocimeter (LDV)

The perpendicular air velocity component, *U*, shall be obtained from Equation 7.8.1.

$$U = (f_D)(d_f) \tag{7.8.1}$$

where

U = airflow velocity in direction shown, m/s (fpm)
f_D = measured Doppler burst frequency, Hz
d_f = fringe spacing = $\lambda/[2\sin(\kappa)]$, m (ft)
λ = wavelength of laser light , m (ft)
κ = half of the angle between the two intersecting laser beams, rad (deg)

8. AIRFLOW MEASUREMENT DUCT FEATURES AND COMPONENTS

8.1 Overview. Features and components used in the airflow measurement test ducts that are described in Section 9 include static pressure taps, piezometer rings, flow straighteners, transition pieces, and variable air supply or exhaust systems.

8.2 Static Pressure Taps. Unless otherwise specified, static pressure taps shall be constructed as defined in Figure 8.2.1 and shall be located around the duct perimeter in a measurement plane with (a) one pressure tap located on each surface of a rectangular duct and centered within ±10% of the width of the surface, or (b) four pressure taps shall be located with one pressure tap at each 90 degrees of circumference within ±10 degrees.

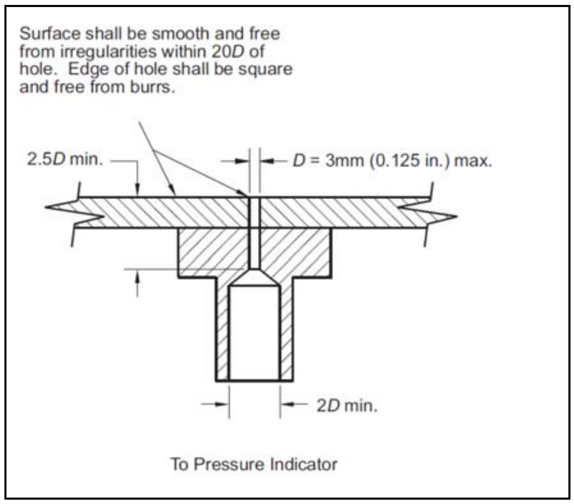

Figure 8.2.1 Static Pressure Tap Construction Requirements

8.3 Piezometer Ring

8.3.1 Piezometer Ring Requirements. Piezometer ring is the name given to the static pressure manifolds that provide an average static pressure at a given measurement plane. Unless otherwise specified in the test plan in Section 5.1, piezometer rings shall be installed as illustrated in Figure 8.3.1 with the following constraints:

a. The four tubing segments (A + B) shall have equal lengths within ±10%.

b. The four tubing segments C shall have equal lengths within ±10%.

c. The tubing segments (D + E) and (F + G) shall have equal lengths within ±10%.

d. The tubing segments (H + J) and (K + L) shall have equal lengths within ±10%.

e. The four tubing segments M shall have equal lengths within ±10%.

f. The four tubing segments N shall have equal lengths within ±10%.

g. Tubing shall be made from metal or plastic with enough strength to operate at 31 kPA (199 psig) to 35 kPa (227 psig) to pass the installed piezometer ring pressure leak test procedures prescribed in Section 8.3.2.

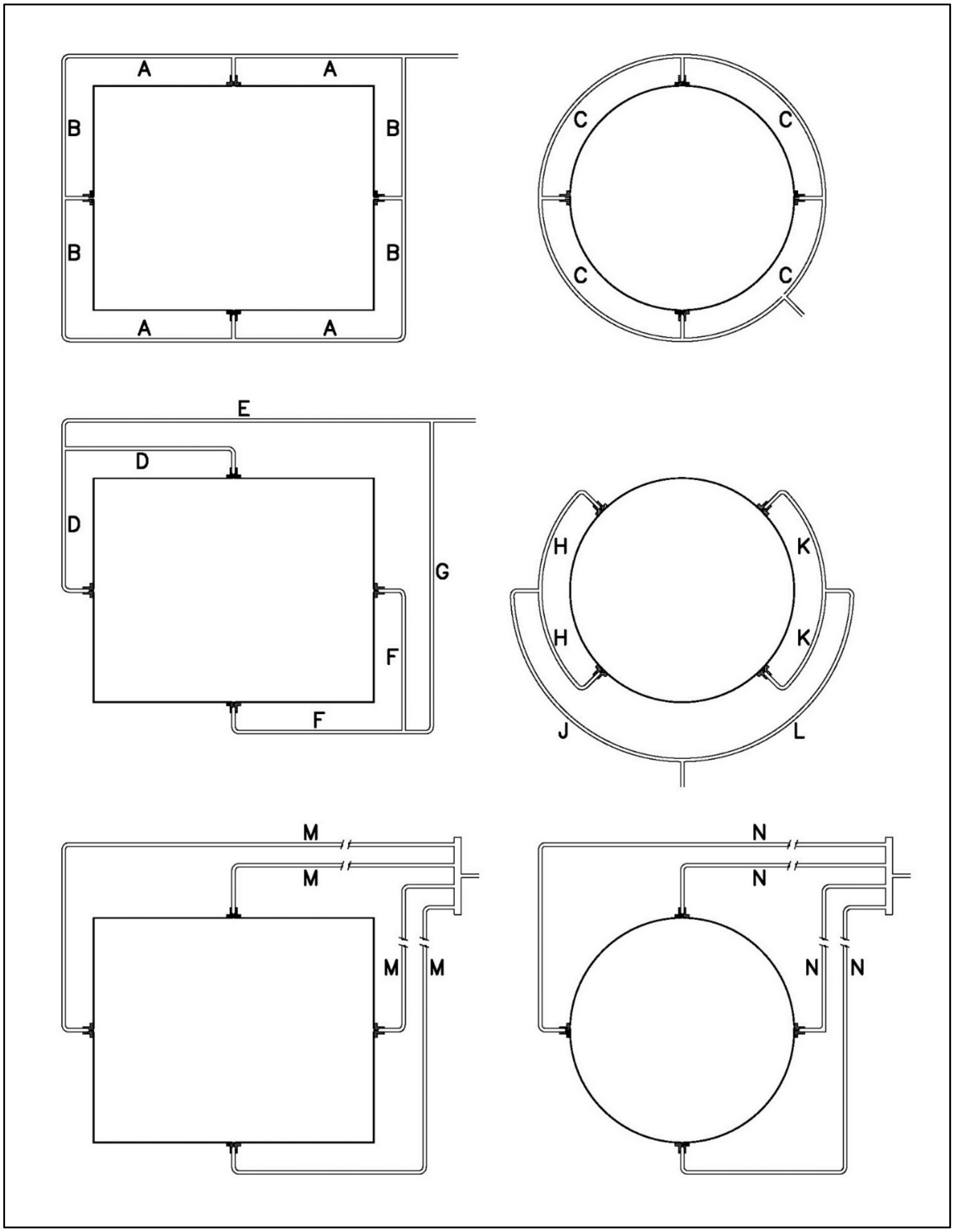

Figure 8.3.1: Piezometer Ring Connection Alternatives

8.3.2 Piezometer Ring Leak Test. Leak test each installed piezometer ring assembly as prescribed in Sections 8.3.2.1, 8.2.3.2, 8.2.3.3, and 8.2.3.4 unless otherwise specified by the test plan in Section 5.1.

8.3.2.1 Disconnect each barometric pressure sensor and each differential pressure sensor in the installed piezometer ring assembly. Use one of the open tube ends to pressurize the assembly in accordance with 8.3.2.2 and 8.3.2.3. Plug the remaining open tube ends.

8.3.2.2 Connect the open end of the tube in to a source of regulated compressed air or compressed nitrogen as illustrated in Figure 8.3.2 that has (a) an integral pressure gauge at the connection and (b) a dew point temperature no more than -40 °C (-40 °F) at a pressure no less than 34 kPa (5 psig) and no more than 69 kPa (10 psig).

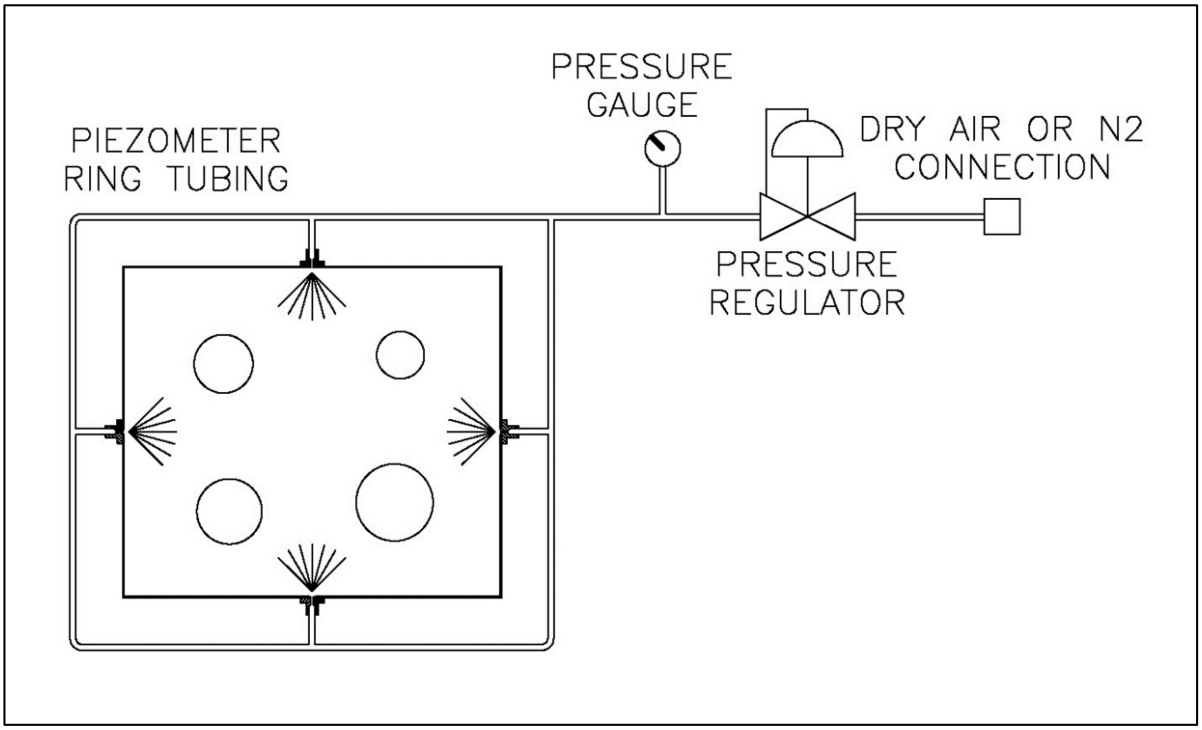

Figure 8.3.2. Piezometer Leak Test Setup Illustration

8.3.2.3 Apply a leak test liquid solution to the perimeter of each tubing connection and fitting in the installed piezometer assembly. Bubbles in the leak test solution indicate leaks. Repair the installed piezometer assembly to eliminate the leaks that are found using this procedure, and repeat this leak test procedure until the installed piezometer ring assembly is leak-free.

8.3.2.4 Release the leak test pressure, disconnect the source of compressed air or compressed nitrogen, and re-install each barometric pressure sensor and each differential pressure sensor.

8.4 Flow Straighteners. Cell-type flow straighteners shall conform to Figure 8.4.1 and the thickness dimension, *y*, shall not exceed 0.005 D_h. Star-type flow straighteners shall conform to Figure 8.4.2. **(Informative Note 1):** Although the term “straightener” is widely used to describe these devices, the replacement term “conditioner” is emerging because “conditioner” more aptly describes the function of these devices. **(Informative Note 2):** For further reading, see Informative Annex A citation A6.

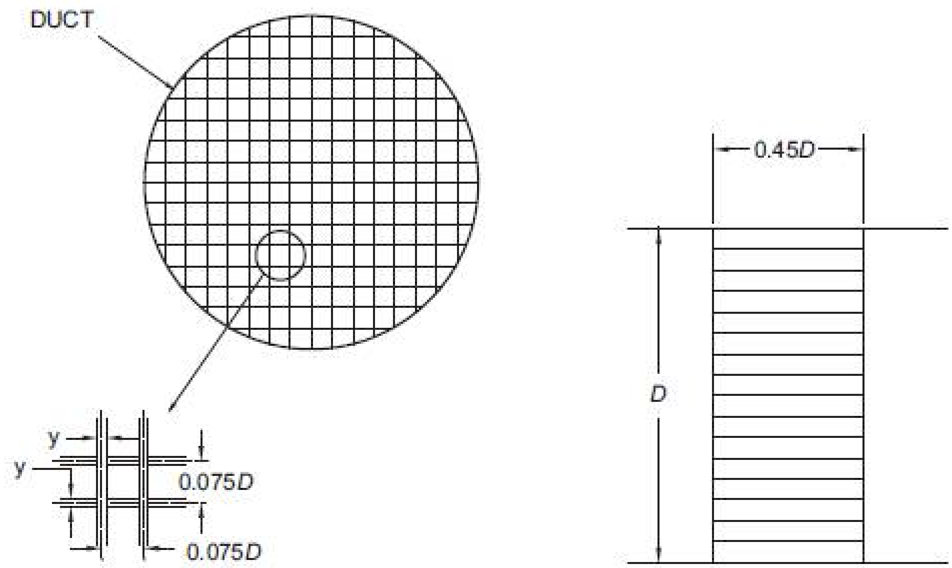

Notes:

1. All dimensions shall be within ±0.005*D* except *y*, which shall not exceed 0.005*D*
2. Cell sides shall be flat and straight. Where *y* > 3 mm (0.125 in.), the leading edge of each segment shall have a chamfer of 1.3 mm (0.05 in.) per side. The method of joining cell segments (such as tack welds) shall be kept to the minimum required for mechanical integrity and shall result in minimum protusion into the fluid stream.

Figure 8.4.1: Cell Type Flow Straightener

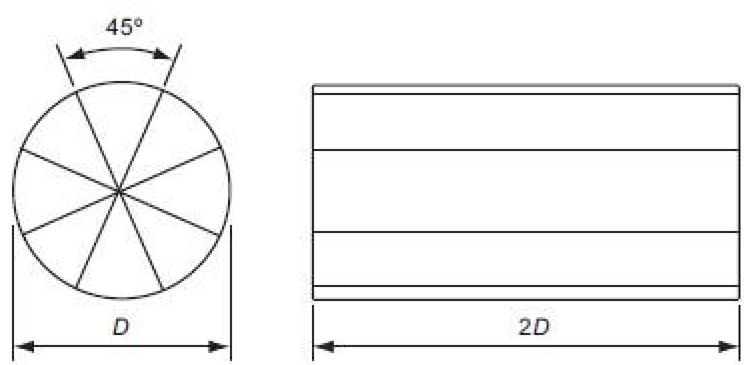

The star straightener will be constructed of eight radial blades of length equal to $2D_4$ (with a ±1% tolerance) and of thickness not greater than $0.007D_4$. The blades will be arranged to be equidistant on the circumference with the angular deviation being no greater than 5° between adjacent plates.

Figure 8.4.2: Star-Type Flow Straightener

8.5 Transformation Pieces. Transformation pieces used to connect rectangular units under test (UUTs) to round test ducts or chambers, or round UUTs to rectangular test ducts or chambers shall be made in accordance with Figure 8.5.1.

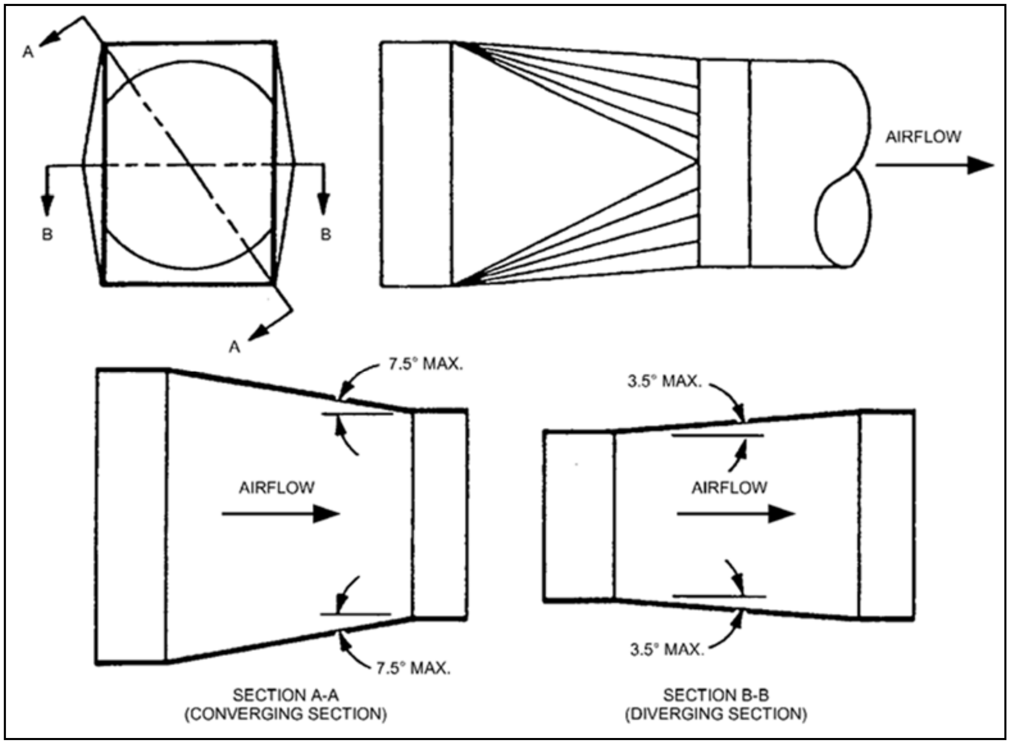

Figure 8.5.1: Transformation Pieces

9. AIRFLOW MEASUREMENT METHODS

9.1 Constraint on All Airflow Measurement Methods. A selected airflow measurement plane shall exceed 7.5 geometrically equivalent diameters downstream of an obstruction or any change in the airflow direction and shall exceed 3 geometrically equivalent diameters upstream of an obstruction or change in the airflow direction unless otherwise specified by the airflow measurement instrument manufacturer. For a rectangular duct with interior width and height dimensions equal to *"a"* and *"b"* respectively, the geometrically equivalent diameter shall be obtained from Equation 9.1.1. For a round duct, the geometrically equivalent diameter, D_E, is equal to the interior diameter, *D*.

$$D_E = \sqrt{\frac{4ab}{\pi}} \tag{9.1.1}$$

9.2 Pitot-Static Tube Airflow Measurement Methods. The airflow measurement methods in this section are based upon Pitot-static tube measurement principles.

9.2.1 Pitot-Static Tube Traverse Airflow Measurement. Figure 9.2.1 shows an example Pitot-static tube construction and the connections to manometers or electronic pressure transducers. Sections 9.2.1, 9.2.2, and 9.2.3 describe three different methods to determine gas velocity at measurement points in a gas stream by measuring total and static pressures. Pitot-static tubes shall be aligned within ±10 degrees of the airflow direction, and any misalignment shall be included in the uncertainty estimate. **(Informative Note 1):** Negative dynamic (or velocity) pressure readings are a clear indication that the Pitot-static tube is not properly aligned with the direction of air velocity. **(Informative Note 2):** Severe errors are also possible even if negative pressure readings are not observed. It is critical that the flow direction be known and the probe be properly aligned with the flow direction. **(Informative Note 3):** Traversing techniques have also been applied to other velocity measurement methods, including hot-wire or hot-film anemometers.

The process of sequentially positioning a single Pitot-static tube at different measuring points within a measurement plane to measure air velocities is called a Pitot-static tube traverse. Prescribed Pitot-static traverse measuring points within a measurement plane are shown in Figure 9.2.2 for both rectangular and round ducts.

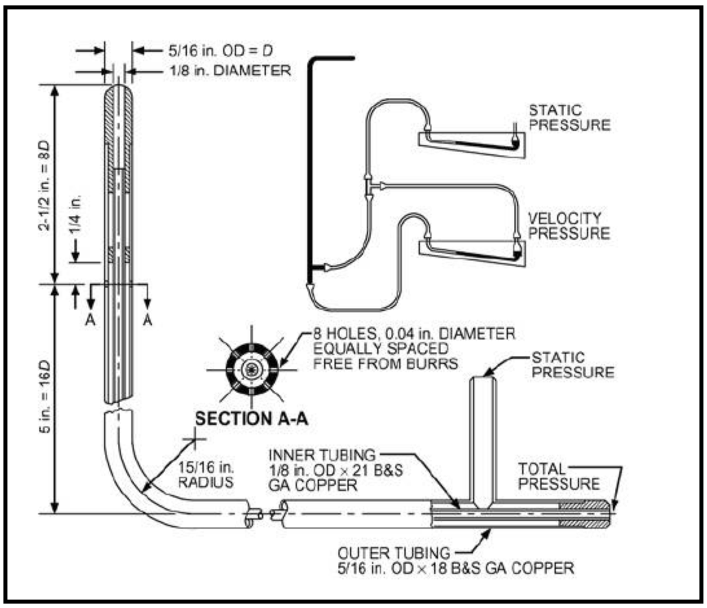

Figure 9.2.1: An Example of Pitot-Static Tube Construction and Connections

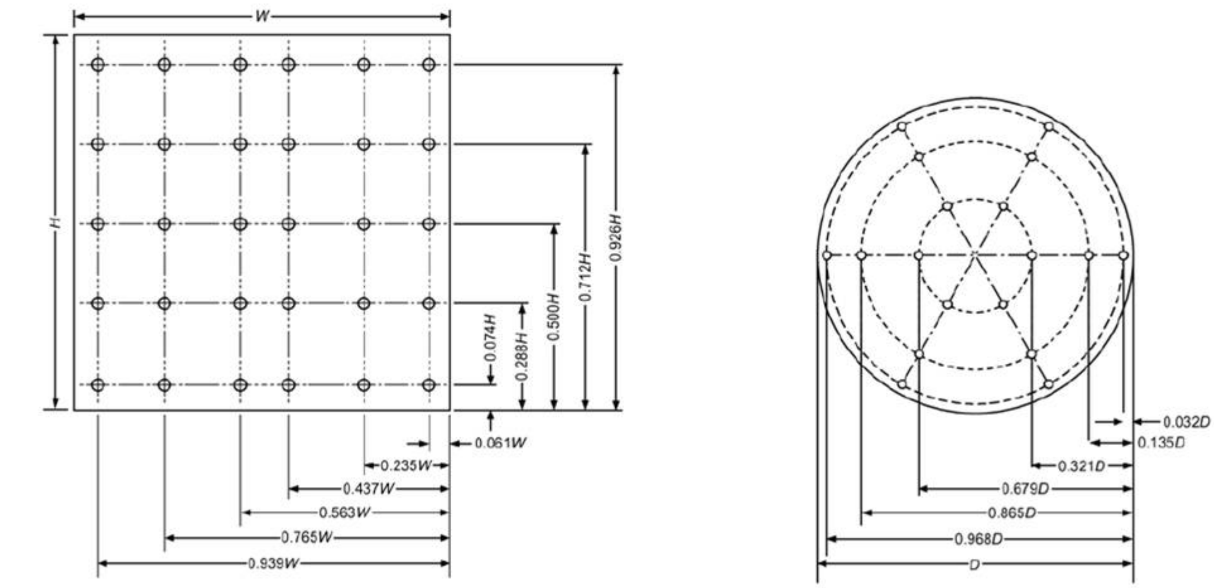

Duct Dimensions	No. of Points for Traverse Lines	Position Relative to Inner Wall
18 in. < H, W < 30 in.	5	0.074, 0.288, 0.500, 0.712, 0.926
30 in. ≤ H, W ≤ 36 in.	6	0.061, 0.235, 0.437, 0.563, 0.765, 0.939
H, W > 36 in.	7	0.053, 0.203, 0.366, 0.500, 0.634, 0.797, 0.947

Log-Tchebycheff Rule for Rectangular Ducts

Note: Example duct has 5 × 6 (H × W) measurement pattern, as for rectangular duct of 24 × 30 in.

No. of Measuring Points per Diameter	Position Relative to Inner Wall
6	0.032, 0.135, 0.321, 0.679, 0.865, 0.968
8	0.021, 0.117, 0.184, 0.345, 0.655, 0.816, 0.883, 0.979
10	0.019, 0.077, 0.153, 0.217, 0.361, 0.639, 0.783, 0.847, 0.923, 0.981

Log-Linear Rule for Circular Ducts

Figure 9.2.2 Pitot-Tube Traverse Measuring Points for Rectangular Ducts and Round Ducts

9.2.1.1 Velocity Pressure. The total pressure, P_{ti}, is the sum of the static pressure, P_{si}, and the velocity pressure, P_{vi}, at each traverse measurement point. The velocity pressure at each measurement location shall be obtained from Equation 9.2.1.1.

$$P_{vi} = P_{ti} - P_{si} \qquad 9.2.1.1$$

9.2.2.2 Average Velocity Pressure. The average velocity pressure, P_{va}, shall be obtained from Equation 9.2.2.2.

$$P_{va} = \left(\frac{\sum_{i=1}^{N}\sqrt{P_{vi}}}{N}\right)^2 \qquad 9.2.1.2$$

9.2.2.3 Average Air Velocity. The average air velocity shall be obtained from Equation 9.2.2.3 in SI units or from Equation 9.2.2.4 in I-P units.

$$V_a = K\sqrt{\frac{2P_{va}}{\rho}} \qquad 9.2.1.3$$

$$V_a = 1097.8K\sqrt{\frac{P_{va}}{\rho}} \qquad 9.2.1.4$$

9.2.2.4 Volumetric Airflow. The volumetric airflow at the measurement plane shall be obtained from Equation 9.2.2.5.

$$Q = V_a A \qquad 9.2.2.5$$

9.2.2 Self-Averaging Array Airflow Measurement. Self-averaging arrays consist of multiple bifurcated or extruded tubes spread out over a measurement plane that have holes to sample and self-average both total and static pressure across the measurement plane. The self-averaged total pressure is connected to one side of a differential pressure transducer, and the self-averaged static pressure is connected to the other side of the same pressure transducer. **(Informative Note):** For user information, see Informative Annex E Section E5.

9.2.2.1 Average Velocity Pressure. The average total pressure, velocity pressure, P_{va}, in the measurement plane shall be obtained from Equation 9.2.2.1.

$$P_{va} = P_{ta} - P_{sa} \quad 9.2.2.1$$

9.2.2.2 Average Air Velocity. The average air velocity shall be obtained from Equation 9.2.2.2 in SI units or from Equation 9.2.2.3 in I-P units.

$$V_a = K\sqrt{\frac{2P_{va}}{\rho}} \quad 9.2.2.2$$

$$V_a = 1097.8K\sqrt{\frac{P_{va}}{\rho}} \quad 9.2.2.3$$

9.2.2.3 Volumetric Airflow. The volumetric airflow at the measurement plane shall be obtained from Equation 9.2.2.4.

$$Q = V_a A \quad 9.2.2.4$$

9.2.3 Self-Averaging Probe Airflow Measurement. Self-averaging probes include multiple total and static pressure ports along a straight line or around a circumference within the airstream. The self-averaged total pressure is connected to one side of a differential pressure transducer, and the self-averaged static pressure is connected to the other side of the same pressure transducer.

9.2.3.1 Average Velocity Pressure. The average total pressure, velocity pressure, P_{va}, in the measurement plane shall be obtained from Equation 9.2.3.1.

$$P_{va} = P_{ta} - P_{sa} \quad 9.2.3.1$$

9.2.3.2 Average Air Velocity. The average air velocity shall be obtained from Equation 9.2.3.2 in SI units or from Equation 9.2.3.3 in I-P units.

$$V_a = K\sqrt{\frac{2P_{va}}{\rho}} \quad 9.2.3.2$$

$$V_a = 1097.8K\sqrt{\frac{P_{va}}{\rho}} \quad 9.2.3.3$$

9.2.3.4 Volumetric Airflow. The volumetric airflow at the measurement plane shall be obtained from Equation 9.2.3.4.

$$Q = V_a A \quad 9.2.3.4$$

9.3 Single and Multiple Nozzle Airflow Methods

9.3.1 ASHRAE Nozzle Geometry. Figure 9.3.1.1 prescribes geometric proportions and specifications for installed nozzles. Nozzles that are constructed in accordance with Figure 9.3.1.1 require no calibration.[6] Multiple nozzle chambers use the nozzle version without throat taps.

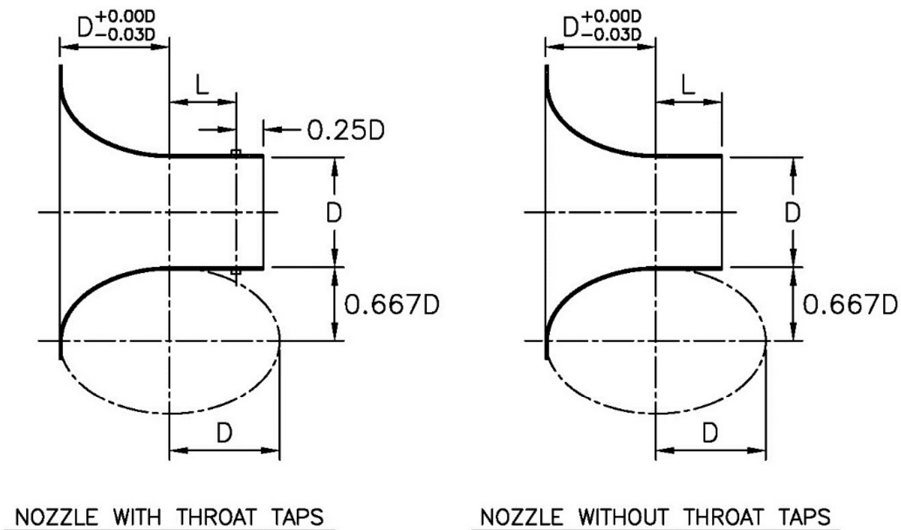

1. The nozzle shall have a cross−section consisting of an elliptical nozzle and a cylindrical portion as shown. The elliptical portion is the nozzle inlet and the cylindrical portion is the nozzle throat.
2. The dimensions of the elliptical portion are shown.
3. Arcs shall smoothly meet and blend with the adjacent arc or cylindrical portion.
4. Nozzle throat dimension L shall be 0.6D ± 0.005D.
5. Nozzle throat shall be cylindrical within ± 0.001D.
6. Nozzle surface roughness shall be not more than ± 0.001D peak−to−peak.

Figure 9.3.1.1 Nozzle Geometry

9.3.2 Nozzle Airflow Test Setup Construction Requirements.

9.3.2.1 Cross Sections of Test Chambers and Test Ducts. The cross section of test chambers and text ducts shall be round or rectangular. Transformation pieces described in Section 8.3.3 shall be used to connect rectangular units under test (UUTs) to round test chambers or test ducts, or to connect round UUTs to rectangular test chambers or test ducts. For a rectangular test chamber or test duct with interior width and height dimensions equal to *"a"* and *"b"* respectively, the geometrically equivalent diameter shall be obtained from Equation 9.1.1. For a round test chamber or test duct, the geometrically equivalent diameter, $D_{E,}$ is equal to the interior diameter, *D*.

9.3.2.2 Nozzle Throat Velocity. The throat velocity of each nozzle shall exceed 3000 fpm (15 m/s).

9.3.2.3 Nozzle Chamber Size Requirement. In nozzle chambers, the chamber interior geometrically equivalent diameter shall be greater than 2 times the geometrically equivalent diameter, D_E, of the air inlet duct.

9.3.2.4 Longitudinal Spacing Requirements. In nozzle chambers, the minimum distance between the upstream screens and the nozzle inlets shall be the greater of $0.5D_E$ or $1.5d_L$ where d_L is the largest nozzle throat diameter.

9.3.2.5 Radial Spacing Requirement for Adjacent Nozzles. In multiple nozzle chambers, the centerline-to-centerline distance between adjacent nozzles shall exceed $3d_L$ where d_L is the largest nozzle throat diameter.

9.3.2.6 Radial Spacing Requirement. The distance from the centerline of any nozzle to the nearest interior wall shall exceed 1.5 times its throat diameter, *d*.

9.3.2.7 Single Nozzle Duct Throat Diameter Limit. The ratio of nozzle throat diameter, *d*, to the geometrically equivalent diameter of the inlet duct, D_E, shall not exceed $0.53D_E$.

9.3.2.8 Airflow Settling Means Requirements for Nozzle Chambers. An airflow settling means, consisting of at least 3 screens or perforated sheets having open areas of 40% to 65%, shall be installed in test chambers where indicated on the test setup figures in Sections 9.3.3 and 9.3.4. The maximum velocity in multiple nozzle chambers at a distance of $0.1D_E$ downstream of the upstream settling means shall be measured and shall not exceed the average velocity by more than 20% unless the maximum velocity is less than 2 m/s (400 fpm). **(Informative Note 1):** Where located upstream of the measurement plane, the purpose of the settling means is to provide a uniform flow ahead of measurement plane. Where located downstream of the measurement plane, the purpose of the settling means is absorb the kinetic energy to allow expansion to simulate expansion into an unconfined space. **(Informative Note 2):** Recommend using square mesh round wire screens upstream of the measurement plane and perforated sheets downstream. **(Informative Note 3):** Recommend using three or four screens with decreasing percent of open area in the direction of airflow.

9.3.3 Single Nozzle Duct Test Setup. Figure 9.3.3.1 shows the single nozzle duct test setup that is within the scope of this standard.

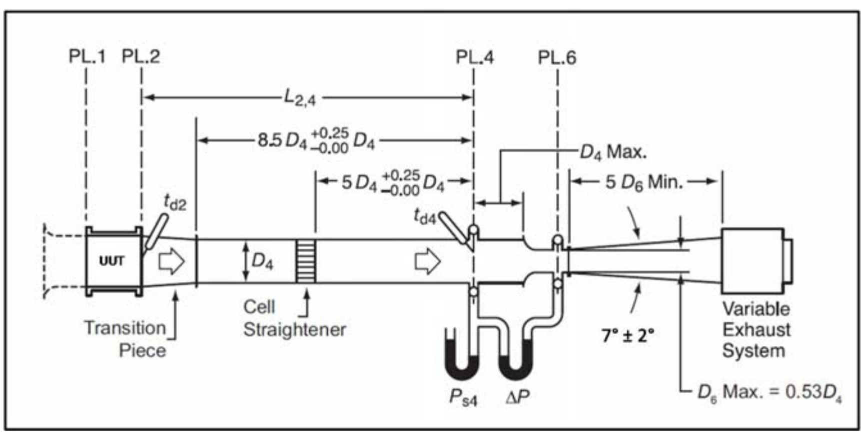

Figure 9.3.3.1 Single Nozzle Duct Test Setup

9.3.4 Single and Multiple Nozzle Chamber Design. Figure 9.3.4.1 shows the construction requirements for a single or multiple nozzle chamber.

9.3.4.1 Chamber Size. The chamber geometrically equivalent diameter shall be sized so that the maximum average air velocity is 2 m/s (400 fpm).

9.3.4.2 Upstream Settling Means Verification Test. The maximum velocity at a distance of 0.1D downstream of the upstream settling means shall be measured and shall not exceed the average velocity by more than 20%.

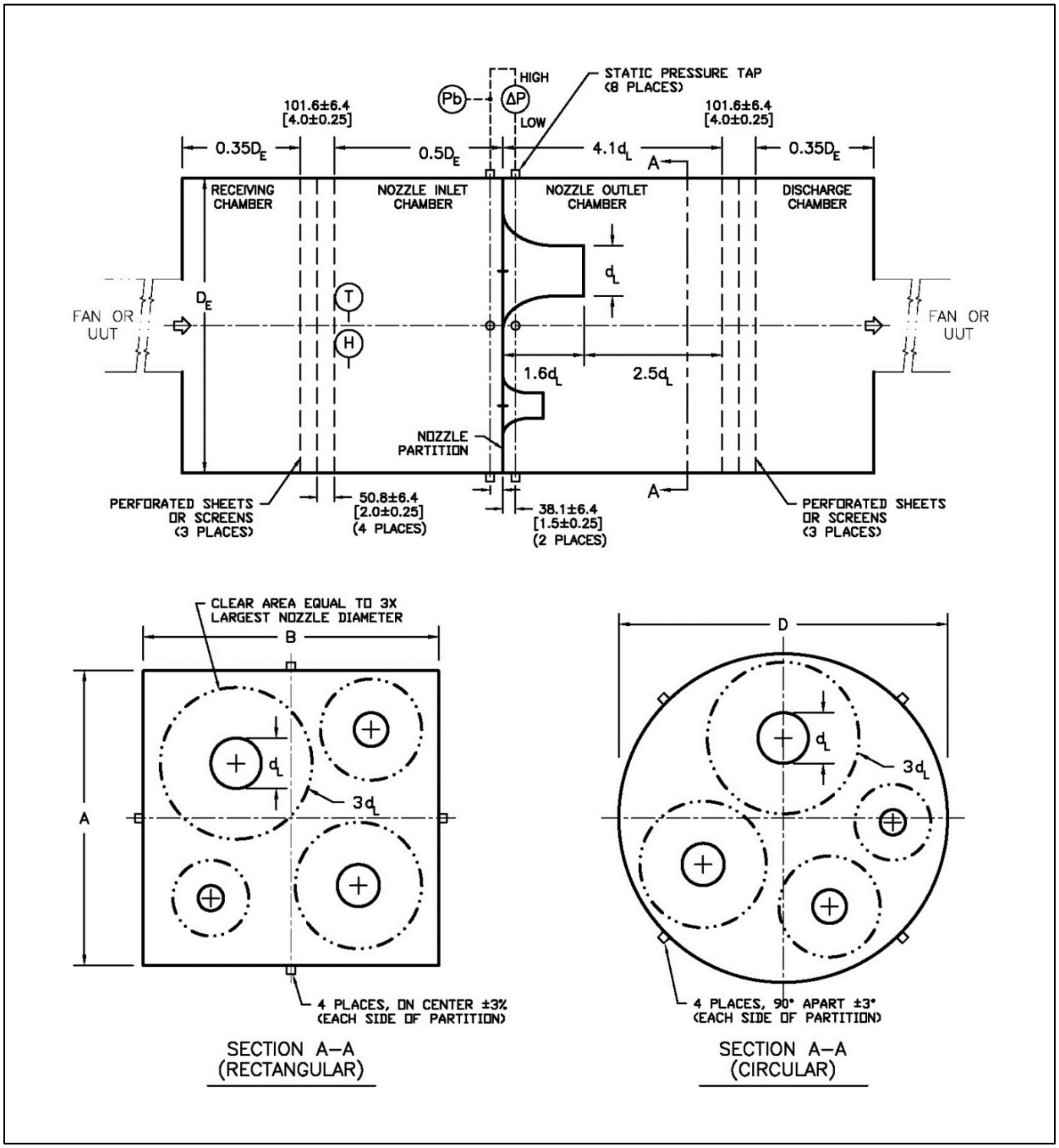

Figure 9.3.4.1. Single or Multiple Nozzle Chamber Construction Requirements

9.3.5 Nozzle Airflow Calculations. ASME PTC 19.5[7] and ASME MFC-3M[8] describe measurement of fluid flow in pipes using orifices, flow nozzles, and venturi tubes, including construction proportions and port locations. Single nozzle airflow calculation procedures follow the ASME procedures. Multiple nozzle airflow calculations use a discharge coefficient equation and assertions that are based upon the findings of an ASHRAE research paper.[6]

Calculating a volumetric airflow rate for a single nozzle requires iteration because the discharge coefficient, *C*, is a function of the Reynolds number which is a function of the average air velocity, and the average air velocity is not known until the volumetric airflow rate has been determined. ASME PTC 19.5[7] includes an example of this iterative procedure on page 25.

9.3.5.1 Measurements. Measurements required for this nozzle airflow calculations shall be:

a. Inlet duct geometrically equivalent diameter, D_E, m (ft)
b. Throat diameter, d, m (ft)
c. Inlet absolute pressure, p_1, Pa (psia)
d. Differential pressure, $\Delta p = (p_1 - p_2)$, Pa (psia)
e. Inlet temperature, t_1, °C (°F)
f. Inlet humidity measurement in the form of relative humidity, dew point, or wet bulb temperature.

9.3.5.2 Thermodynamic Properties of Air. Nozzle inlet density and viscosity for dry and moist air shall be obtained from ASHRAE RP-1485[1] using nozzle inlet absolute pressure, temperature, and humidity.

9.3.5.3 Single Nozzle Airflow Calculations

9.3.5.3.1 Single Nozzle Duct and Chamber Diameter. Single nozzle inlet duct hydraulic diameter, D_h, shall be obtained from dimensional measurements. For a round duct, D_h is equal to the interior inlet diameter. For a rectangular duct, the hydraulic diameter shall be obtained from Equation 9.3.5.1.

$$D_h = \frac{4ab}{(a+b)} \qquad 9.3.5.1$$

where

D_h = hydraulic diameter, m (ft)
a = interior width, m (ft)
b = interior height, m (ft)

9.3.5.3.2 Single Nozzle Reynolds Number. The Reynolds number shall be obtained from Equation 9.3.5.2.

$$Re_D = \frac{\rho_1 V D_h}{\mu_1} \qquad 9.3.5.2$$

where

ρ_1 = inlet air density, kg/m³ (lb$_m$/ft³)
V = average throat air velocity, m/s (ft/s)
D_h = hydraulic diameter, m (ft)
μ_1 = inlet air dynamic viscosity, Ns/m² (lb$_m$/s-ft)

9.3.5.3.3 Single Nozzle Beta Ratio. The single nozzle beta ratio shall be obtained from Equation 9.3.5.3. If airflow operating temperatures are not the same as the airflow operating temperatures during calibration, parameters d, D_h, and β shall be corrected to account for thermal expansion in accordance with ASME PTC 19.5[7] Section 3-10.

$$\beta = \left(\frac{d}{D_h}\right) \qquad 9.3.5.3$$

9.3.5.3.4 Single Nozzle Volumetric Airflow Rates. Single nozzle volumetric airflow rates shall be obtained from Equation 9.5.3.4 in SI units or Equation 9.5.3.5 in I-P units.

$$Q = CA\varepsilon\sqrt{\frac{2(\Delta p)}{\rho_1(1-\beta^4)}} \qquad 9.5.3.4$$

where

Q = volumetric flow rate, m^3/s
C = discharge coefficient, dimensionless
ε = expansibility factor, dimensionless
A = nozzle throat area, m^2
ρ_1 = nozzle inlet gas density, kg/m^3
Δp = nozzle differential pressure, Pa
β = d/D_h, dimensionless

$$\mathbf{Q = CA\varepsilon\sqrt{\frac{2g_c(\Delta p)}{\rho_1(1-\beta^4)}}}$$ .... **9.5.3.5** ....

where

Q = volumetric flow rate, cfm
C = discharge coefficient, dimensionless
ε = expansibility factor, dimensionless
g_c = gravitational constant, 32.174 $(lb_m \cdot ft)/(lb_f \cdot s^2)$
A = nozzle throat area, ft^2
ρ_1 = nozzle inlet gas density, lb_m/ft^3
Δp = nozzle differential pressure, psia
β = d/D_h, dimensionless

9.3.5.3.5 Single Nozzle Limits of Use. The nozzle geometry in Figure 9.3.1.1 conforms to ASME's long radius nozzle type geometry requirements, and the throat velocity requirement in Section 9.3.2 confirms that the single nozzle will be operating within the long radius nozzle limits prescribed by ASME.

9.3.5.3.6 Single Nozzle Expansibility Factor. The dimensionless expansibility factor, ε, for a long radius nozzle shall be obtained from Equation 9.3.5.6.

$$\varepsilon = \left[r^{\frac{2}{\gamma}}\left(\frac{\gamma}{\gamma-1}\right)\left(\frac{1-r^{\frac{\gamma-1}{\gamma}}}{1-r}\right)\left(\frac{1-\beta^4}{1-\beta^4 r^{\frac{2}{\gamma}}}\right)\right]^{1/2} \qquad 9.3.5.6$$

where

r = absolute pressure ratio (p_1/p_2), dimensionless
γ = ratio of specific heat at constant pressure to specific heat at constant volume

9.3.5.3.7 Single Nozzle Discharge Coefficient. The dimensionless discharge coefficient, C, for a long radius nozzle is a function of β and the Reynolds number based upon the nozzle inlet diameter. The discharge coefficient for the nozzle geometry defined in Section 9.3.1 shall be obtained from Equation 9.3.5.7.

$$C = 0.9965 - (0.00653\beta^{0.5})\left(\frac{10^6}{Re_D}\right)^{0.5} \qquad 9.3.5.7$$

9.3.5.3.8 Single Nozzle Calculation Iteration. The Reynolds number shall be obtained from 9.3.5.2, but the average velocity is not known until the volumetric airflow rate has been determined. Iteration is required to determine the gas mass flow rate. Choose $C = 1.0$ to begin the iterative calculation procedure. Iteration shall continue until the calculated discharge coefficient, C, matches the previous discharge coefficient within ±0.005.

9.3.5.4 Multiple Nozzle Airflow Calculations. The multiple nozzle airflow calculations follow the ASME procedures but use a discharge coefficient equation and assertions that are based upon the findings of an ASHRAE research paper.[6]

9.3.5.4.1 Multiple Nozzle Reynolds Number. The Reynolds number shall be obtained from Equation 9.3.5.8.

$$Re_d = \frac{\rho_1 V d}{\mu_1} \qquad 9.3.5.8$$

where
- ρ_1 = nozzle inlet air density, kg/m³ (lbm/ft³)
- V = nozzle throat average air velocity, m/s (ft/s)
- d = nozzle throat diameter, m (ft)
- μ_1 = nozzle inlet dynamic viscosity, Ns/m² (lbm/s-ft)

9.3.5.4.2 Multiple Nozzle Beta Ratio. Based upon Reference 6, $\beta = 0$ for multiple nozzle chambers.

9.3.5.4.3 Multiple Nozzle Limits of Use. The nozzle geometry in Figure 9.3.1.1 fits into ASME's long radius nozzle type, and the throat velocity requirement in Section 9.3.2 confirms that the single nozzle will be operating within the long-radius nozzle limits prescribed by ASME.

9.3.5.4.4 Multiple Nozzle Expansibility Factor. The dimensionless expansibility factor, ε, for a long radius nozzle is shown in Equation 9.3.5.9.

$$\varepsilon = \left[r^{\frac{2}{\gamma}}\left(\frac{\gamma}{\gamma-1}\right)\left(\frac{1-r^{\frac{\gamma-1}{\gamma}}}{1-r}\right)\left(\frac{1-\beta^4}{1-\beta^4 r^{\frac{2}{\gamma}}}\right)\right]^{1/2} \qquad 9.3.5.9$$

where
- r = absolute pressure ratio (p_1/p_2), dimensionless
- γ = ratio of constant pressure to constant volume specific heat

For multiple nozzle test chambers, substitution of $\gamma = 1.4$ and $\beta = 0$ into Equation 9.3.5.9 results in Equation 9.5.3.10. The multiple nozzle expansibility factor shall be obtained from Equation 9.3.5.10.

$$\varepsilon = 1 - 0.548(1 - r) \qquad 9.3.5.10$$

9.3.5.4.5 Multiple Nozzle Discharge Coefficient. Nozzle discharge coefficients shall be calculated for each nozzle in use from Equation 9.3.5.11 using the Reynolds number from Equation 9.3.5.8.

$$C = 0.99855 - \left[\frac{7.006}{\sqrt{Re_d}}\right] + \left[\frac{134.6}{Re_d}\right] \qquad 9.3.5.11$$

An iterative calculation process is required to determine individual nozzle coefficients. Choose $C = 0.98$ to begin the iterative calculation procedure. Iteration shall continue until the calculated discharge coefficient, C, matches the previous discharge coefficient within ±0.005.

9.3.5.4.6 Multiple Nozzle Volumetric Airflow Rate. The volumetric airflow rate at the entrance to multiple nozzles shall be obtained from Equation 9.3.5.12 in SI units or from Equation 9.3.5.13 in I-P units where the area is measured at the plane of the throat taps or nozzle exit for nozzles without throat taps.[6]

$$Q = [\sum(CA)]\varepsilon\sqrt{\frac{2\Delta p}{\rho_1}} \qquad \text{m}^3/\text{s (SI)} \qquad 9.5.3.12$$

$$Q = 1097.8[\sum(CA)]\varepsilon\sqrt{\frac{\Delta p}{\rho_1}} \qquad \text{ft}^3/\text{m (I-P)} \qquad 9.5.3.13$$

9.3.5.4.7 Standard Airflow Rate. The standard airflow rate shall be calculated in accordance with Section 4.5 using Equation 9.3.5.14 in SI units or Equation 9.3.5.15 in SI units.

$$\text{Standard Cubic Meters/Second} = \frac{\rho_1 Q}{1.202} \qquad \text{(SI)} \qquad 9.3.5.14$$

$$\text{Standard Cubic Feet/Minute (SCFM)} = \frac{\rho_1 Q}{0.075} \qquad \text{(I-P)} \qquad 9.3.5.15$$

9.3.5.4.8 Mass Airflow Rate. The mass airflow rate shall be obtained from Equation 9.3.5.16.

$$\dot{m} = \rho_1 Q \qquad \text{kg/s (lb}_\text{m}\text{/min)} \qquad 9.3.5.16$$

9.4 Thermal Dispersion Arrays. Review Section 9.1. A thermal dispersion sensor measures air velocity at a single point in an airstream by measuring the heat dispersed from the heated sensor into the airstream. Commercial thermal dispersion arrays include (a) multiple thermal dispersion probes comprised of multiple sensors that are equally-spaced along a straight line, and (b) the associated equipment required for collecting and averaging the individual air velocity measurements to provide the resulting measured average air velocity for display or automated data recording.

Install an array of thermal dispersion probes into a measurement plane in either a rectangular duct or a round duct as prescribed in Figure 9.4.1. In a rectangular duct, X equals the duct height and the tolerance for illustrated dimensions is ±3 mm (±0.12 in.). For a round duct, the tolerance for illustrated positions is ± 5 degrees. **(Informative Note 1):** A thermal dispersion array will indicate positive airflow, even if the airflow is reversed. **(Informative Note 2):** For user information, see Informative Annex E Section E7.

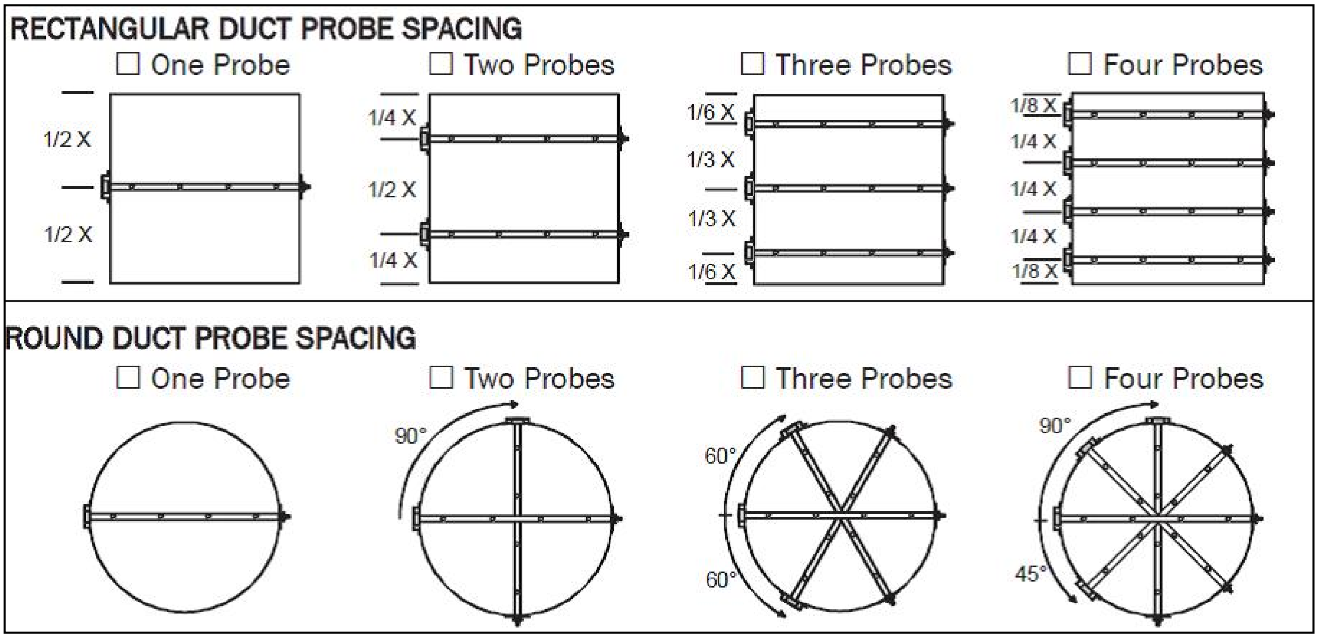

Figure 9.4.1. Thermal Dispersion Probe Locations in Rectangular and Round Ducts

9.5 Vortex-Shedding Arrays. Review Section 9.1. Vortex-shedding arrays are used to determine gas velocities. Piezoelectric methods, strain-gage methods, or hot-film methods are used to sense dynamic pressure variations created by vortex shedding. The operating principle for these flowmeters is based on vortex shedding that occurs downstream of an immersed blunt-shaped solid body. As the airstream passes a blunt-shaped body, the air separates and generates small vortices that are shed alternately along and downstream of each side of the blunt-shaped body. Each vortex-shedding meter is designed to have a known relationship between the Strouhal number and the Reynolds number so that the vortex shedding frequency is a known function of the air velocity over a specified flow velocity range. **(Informative Note):** For further reading, see Informative Annex A citation A6.

9.6 Capture Hoods. Review Section 9.1. Flow capture hoods are portable instruments designed to measure the airflow from diffusers and grilles. A capture hood system consists of a fabric hood and a rigid base assembly that contains the flow sensing equipment. For volumetric airflow measurements, the hood is placed over a diffuser or grille and directs airflow from the outlet or inlet across the flow-sensing manifold in the base of the instrument. The manifold consists of a number of tubes containing upstream and downstream holes in a grid, designed to simultaneously sense and average multiple velocity points across the base of the hood. Airflow from the upstream holes flows through the tubes past a sensor and then exits through the downstream holes. **(Informative Note 1):** Sensors used by different manufacturers include rotating vane anemometers, electronic micromanometers, and thermal anemometers. **(Informative Note 2):** For user information, see Informative Annex E Section E6.

9.7 Tracer Gas Airflow Measurement. Review Section 9.1. Figure 9.7.1 is a schematic of the tracer gas airflow measurement method. This method uses a tracer gas dilution technique that is based upon the principle of mass conservation. Users shall first check the Safety Data Sheet (SDS) to identify health, fire, and exploration hazards for a candidate tracer gas. Tracer gas concentration shall not exceed one tenth of the maximum safe concentration level that is specified in the SDS.

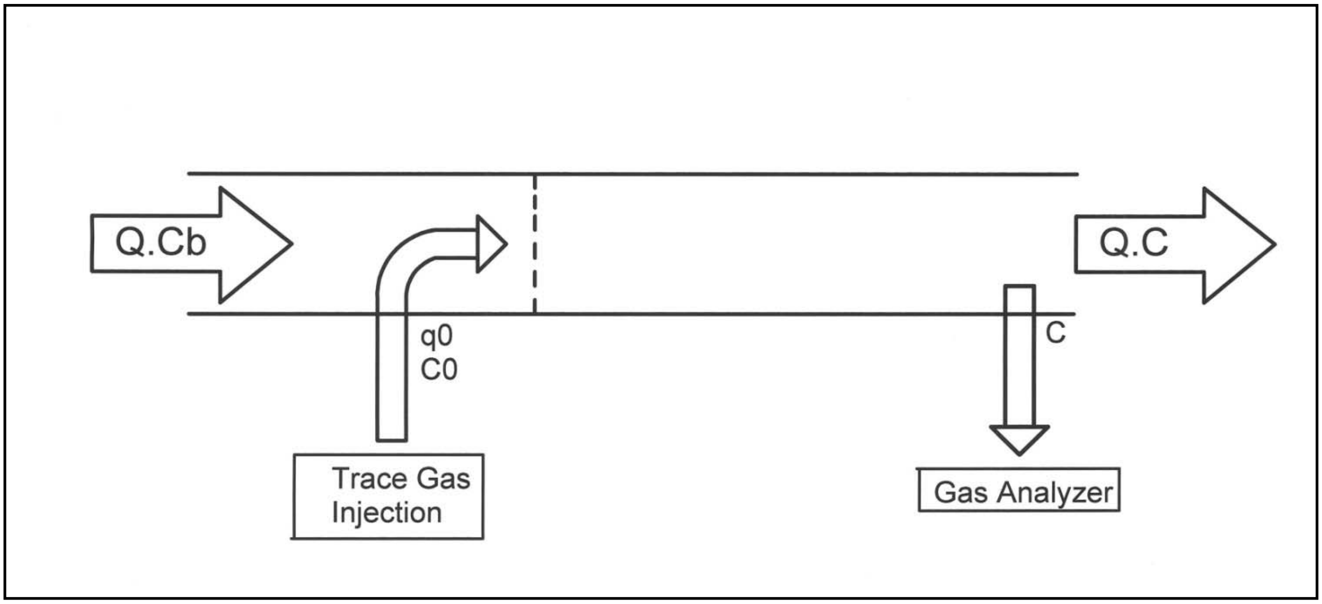

Figure 9.7.1. Tracer Gas Airflow Measurement Schematic

Air flows into the tracer gas test section at an unknown volumetric airflow rate, Q, and a known background concentration, C_b, of the tracer gas if there is any background concentration present upstream of the tracer gas injection location.

A tracer gas is injected into a duct at a known rate, q_0, with known tracer gas concentration, C_0, and disperses into the airstream. Preliminary tests shall be conducted to confirm that the variation of the measured concentration across the measurement plane is less than 10% in accordance with Equation 9.7.1.

$$\frac{\sigma_c^2}{C} < 10\% \qquad 9.7.1$$

where C = the average measured concentration that shall be obtained from Equation 9.7.2

$$C = \frac{\sum_{i=1}^{n} C_i}{n} \qquad 9.7.2$$

where the number of samples, n, shall be at least 10, and

$$\sigma_c^2 = \sum_{i=1}^{n} \frac{(C - C_i)^2}{(n-1)} \qquad 9.7.3$$

If Equation 9.7.1 is 10% or greater, an airflow straightener in accordance with Section 8.4 or an airflow mixer in accordance with ASHRAE Standard 41.1[2] shall be added to the test duct at least 3 diameters or geometrically equivalent diameters upstream of the tracer gas injection plane to increase tracer gas dispersion to satisfy Equation 9.7.1.

The volumetric airflow rate, Q, shall be obtained from Equation 9.7.4 if there is no tracer gas concentration upstream of the tracer gas injection plane or from Equation 9.7.5 if there is a background concentration, C_b, upstream of the tracer gas injection plane.

$$Q = q_0 * \left(\frac{C_0}{C}\right) \qquad 9.7.4$$

$$Q = q_0 * \left(\frac{C_0}{C - C_b}\right) \quad 9.7.5$$

10. MEASUREMENT UNCERTAINTY

10.1 Uncertainty Requirements

An estimate of the measurement uncertainty, performed in accordance with ASME PTC 19.1,[9] shall accompany each air velocity and airflow measurement. Installation effects on the accuracy of the instrument shall be included in the uncertainty estimate for each installation that does not conform to the instrument manufacturer's installation requirements. **(Informative Note):** This procedure is illustrated in the example uncertainty analysis that is provided in Informative Annex B.

10.2. Method to Express Uncertainty

All assumptions, parameters, and calculations used in estimating uncertainty shall be clearly documented prior to expressing any uncertainty values. Uncertainty shall be expressed as:

$$v = \bar{X}_m \pm U_{\bar{X}} \ (P\%) \quad (10.2.1)$$

where:

v = the variable that is a measurement or a calculated result
$\bar{X}_m$ = the best estimate of the true value
$U_{\bar{X}}$ = the uncertainty estimate for the variable
P = the confidence level, percent

(Informative Note): For example: mass airflow = 152.3 kg/s $\pm$ 0.8 kg/s; 95% [1.209 lb_m/h ± 0.006 lb_m/h; 95%] states that the best value for mass airflow is believed to be 152.3 kg/s (1.209 lb_m/h) with a 95% probability that the true value lies within $\pm$ 0.8 kg/s (0.006 lb_m/h) of this value.

11. TEST REPORT

11.1 Test Identification

a. Test Report Number if required in the test plan.
b. UUT identification number.
c. Source of gas property data
d. Date, test facility description, start time, and duration of test.
e. Operator identification.
f. Attach a copy of the Test Plan

11.3 Measurement System Description

a. Description, model number, and serial number.
b. Calibration date
c. Operating range.

11.4 Ambient Conditions

a. Ambient temperature, °C (°F).

b. Barometric pressure, kPa (psia) (required if a pressure-sensing device is referenced to atmospheric pressure; not required if a pressure-sensing device is referenced to absolute pressure).

11.5 Test Conditions

a. Pressure of the gas flow entering the flowmeter, kPa (psia).
b. Temperature of the gas flow entering the flowmeter, °C (°F).

11.6 Test Results

a. Standard volumetric airflow, standard m^3/s (scfm) if required by the test plan in Section 5.1.
b. Volumetric airflow at a measured density, m^3/s (cfm) if required by the test plan in Section 5.1.
c. Mass rate of airflow, kg/s (lb_m/h) if required by the test plan in Section 5.1.
d. Uncertainty in standard volumetric airflow, standard m^3/s (scfm) if required by the test plan in Section 5.1.
e. Uncertainty in volumetric airflow at a measured density, m^3/s (cfm) if required by the test plan in Section 5.1.
f. Uncertainty in mass rate of airflow, kg/s (lb_m/h) if required by the test plan in Section 5.1.

12. REFERENCES

1. Herrmann, S., H.-J. Kretzschmar, and D.P. Gatley, ASHRAE RP-1485, *Thermodynamic Properties of Real Moist Air, Dry Air, Steam, Water, and Ice*, 2008, American Society of Heating, Refrigerating and Air-Conditioning Engineers, Atlanta, GA.
2. ANSI/ASHRAE Standard 41.1-2013, *Standard Methods for Temperature Measurement*. American Society of Heating, Refrigerating and Air-Conditioning Engineers, Atlanta, GA.
3. ANSI/ASHRAE Standard 41.3-2014, *Standard Methods for Pressure Measurement*. American Society of Heating, Refrigerating and Air-Conditioning Engineers, Atlanta, GA.
4. ANSI/ASHRAE Standard 41.6-2014*Standard Methods for Humidity Measurement*. American Society of Heating, Refrigerating and Air-Conditioning Engineers, Atlanta, GA.
5. ANSI/ASHRAE Standard 41.11-2014 *Standard Methods for Power Measurement*. American Society of Heating, Refrigerating and Air-Conditioning Engineers, Atlanta, GA.
6. Bohanon, H. R., *Fan Test Chamber-Nozzle Coefficients*, ASHRAE Technical Paper No. 2334, 1975, American Society of Heating, Refrigerating and Air-Conditioning Engineers, Inc., Atlanta, GA 30329 U.S.A.
7. ANSI/ASME PTC 19.5-2004 (R2013), Flow Measurement. ASME, New York, NY. See Note 1.
8. ASME MFC-3M-2004, *Measurement of Fluid Flow in Pipes Using Orifice, Nozzle, and Venturi*. ASME, New York, NY. See Note 1.
    a. ASME MFC-3Ma-2007, Addenda to ASME MFC-3M-2004. ASME, New York, NY. See Note 1.
9. ASME PTC 19.1-2013, Test Uncertainty, ASME, New York, NY

Note 1: References 7 and 8 are only required if using a Nozzle, an Orifice, or a Venturi Tube test method.

(This annex is not part of this standard. It is merely informative and does not contain requirements necessary for conformance to the standard. It has not been processed according to the ANSI requirements for a standard and may contain material that has not been subject to public review or a consensus process. Unresolved objectors on informative material are not offered the right to appeal at ASHRAE or ANSI.)

INFORMATIVE ANNEX A: BIBLIOGRAPHY

A1. *2013 ASHRAE Handbook –Fundamentals,* Chapter 36 – Measurement and Instruments. American Society of Heating, Refrigerating and Air-Conditioning Engineers, Atlanta, GA.

A2. *ANSI/ASHRAE Standard 51-2007, ANSI/AMCA Standard 210-2007, Laboratory Methods of Testing Fans for Rating.*

A3. *Bohanon, H.R., "Fan test chamber-nozzle coefficients."ASHRAE Transactions, Vol. 81, 1975.*

A4. Doebelin, E. O., *Measurement Systems - Application and Design,* Third Edition. 1983. McGraw-Hill Book Company.

A5. ASHRAE 1245-RP Final Report. 2012. Hickman, C., Beck, B. T., Babin, B., *Determining the Effects of Duct Fittings on Volumetric Airflow Measurements*, June 2012.

A6. ANSI/ASHRAE Guideline 2-2010 (RA 2013)*, Engineering Analysis of Experimental Data*. American Society of Heating, Refrigerating and Air-Conditioning Engineers, Atlanta, GA.

A7. NIST Calibration Services for Gas Flow Meters (Piston Prover and Bell Prover Gas Flow Facilities), by John D. Wright and George E. Mattingly; Process Measurements Division, Chemical Science and Technology Laboratory, NIST, August 1998.

A8. Lebbin, Paul, "Experimental and Numerical Analysis of Air, Tracer Gas, and Particulate Movement in a Large Eddy Simulation Chamber," Ph.D. Thesis, Kansas State University, 2006.

(This annex is not part of this standard. It is merely informative and does not contain requirements necessary for conformance to the standard. It has not been processed according to the ANSI requirements for a standard and may contain material that has not been subject to public review or a consensus process. Unresolved objectors on informative material are not offered the right to appeal at ASHRAE or ANSI.)

INFORMATIVE ANNEX B: EXAMPLE OF MULTIPLE NOZZLE AIRFLOW UNCERTAINTY CALCULATIONS

B1 – Background

In this example, a multiple nozzle chamber is used to measure the volumetric airflow through a unit under test (UUT), m^3/s (ft^3/m). To minimize numerical errors in the example calculations shown below, all intermediate calculations throughout this annex have first been processed to more than 5 significant figures and then rounded to about 5 significant figures. Final calculated results have been rounded to 4 significant figures, and the associated uncertainties of the final calculated results have been expressed in no more than 2 significant figures. The multiple nozzle chamber contains one 0.1524 m (6 in.) throat diameter nozzle, one 0.1016 m (4 in.) throat diameter nozzle, one 0.0762 m (3 in.) throat diameter nozzle, and one 0.0508 m (2 in.) throat diameter nozzle. These nozzles are made of aluminum and constructed in accordance with the dimensional requirements in Figure 9.3.1.1. The throat diameter of each of these nozzles was measured at 4 locations using an inside micrometer that is NIST-traceable. The ambient temperature during the measurements was $22\frac{4}{18}$ °C (72 °F). The measurement results showed that each nozzle is at their nominal size within ± 0.0000254 m (± 0.001 in.). No out-of-roundness of the throat diameters is detected visually.

During chamber operations, the inlet air to the nozzles had a dry bulb temperature of $t_1=15\frac{10}{18}$ °C (60 °F) with a measurement uncertainty of $\Delta t1 = 0.014$ °C (0.0252 °F). The inlet air to the nozzles had a wet bulb temperature of $t'_1=15$ °C (59 °F) with a measurement uncertainty of $\Delta t'1 = 0.05$ ºC (0.09 ºF). The measured barometric pressure at the inlet to the nozzle chamber (upstream of the nozzles and downstream of the settling/straightening devices) is $p_1=101.33$ kPa (14.696 psia) with a $\pm 0.01\%$ of reading pressure transducer after a system calibration for a $\Delta p_1=0.01/100*101.33$ kPa $=\pm 0.010133$ kPa ($\Delta p_1=0.01/100*14.696$ psia$=\pm 0.0014696$ psia).

$$p_2= p_1 - \Delta P \quad \text{(SI \& I-P)} \qquad \text{B1.1}$$

To evaluate the uncertainty in C (nozzle discharge coefficient for a multiple nozzle chamber), the uncertainty in ΔP is evaluated in SI units in Equations B1.2 through B1.4 and in I-P units in B1.5 through B1.7.

In SI Units,

$$\Delta P=0.24911\text{kPa with a } \pm 0.14\% \text{ of full scale and a full scale of } 1.2455\text{kPa} \qquad \text{B1.2}$$

$$\Delta(\Delta P) = \pm 0.14/100*1.2455 = \pm 0.001744 \text{ kPa} \qquad \text{B1.3}$$

$$p_2=101.33 \text{ kPa} - 0.24911 \text{ kPa} =101.08 \text{ kPa} \qquad \text{B1.4}$$

In I-P Units,

ΔP=1 in. H_2O conventional = 0.03613 psia with a $\pm$0.14% of full scale and a full scale of 5 in. H_2O conventional pressure transducer B1.5

$$\Delta(\Delta P) = \pm 0.14/100*5 = \pm 0.007 \text{ in. } H_2O = \pm 0.000253 \text{ psia} \quad B1.6$$

$$p_2 = 14.696 \text{ psia} - 1 \text{ in. } H_2O \text{ conventional} = 14.660 \text{ psia} \quad B1.7$$

Note: The example is not meant to be evaluated constantly moving between SI and I-P, though instead sticking with one system. Approximate conversions are often used between I-P and SI with the example being first done in I-P and then converted to get SI values. These approximations are used as the exact conversions and can fill the page with decimal places as seen in Annex C of this document. The conversions used are from B.9 of NIST Guide to the SI.

The multiple nozzle volumetric airflow rate is defined by Equations 9.3.5.12 in SI units and 9.3.5.13 in I-P units.

$$Q = [\sum(CA)]\varepsilon\sqrt{\frac{2\Delta p}{\rho_1}} \qquad \text{m}^3/\text{s (SI)} \qquad 9.5.3.12$$

$$Q = 1097.8[\sum(CA)]\varepsilon\sqrt{\frac{\Delta p}{\rho_1}} \qquad \text{ft}^3/\text{m (I-P)} \qquad 9.5.3.13$$

The uncertainty will be evaluated in the following order:

B2 – Uncertainty in Areas (A_x)
B3 – Uncertainty in conversion factor of 1097.8 (for I-P only)
B4 – Uncertainty in ε
B5 – Uncertainty in Density (ρ_1)
B6 – Uncertainty in Viscosity
B7 – Uncertainty in Re_x and V_x
B8 – Uncertainty in C
B9 – Uncertainty in $\sum(CA)$
B10 – Uncertainty in Q (the goal here: the measurement uncertainty for this multiple nozzle airflow measurement)

B2 – Uncertainty in Areas (A_x)

The uncertainty in A (nozzle throat area) needs to be evaluated.

Area of a circle $A_x = \frac{\pi {D_{Nx}}^2}{4}$ B2.1

Table B2-1. Nozzle Throat Area

Nozzle Number	Nozzle Throat Diameter	Nozzle Throat Areas	
		SI	I-P
		m^2	ft^2
1	0.1524 m (6 in.)	0.018242	0.19635
2	0.1016 m (4 in.)	0.0081073	0.087267
3	0.0762 m (3 in.)	0.0045604	0.049087
4	0.0508 m (2 in.)	0.0020268	0.021817

$$\Delta A_x = \pm\sqrt{\left(\frac{\partial A_x}{\partial D_{Nx}} \times \Delta D_{Nx}\right)^2} \qquad \text{B2.2}$$

Note: That while π is not known exactly, the 15 significant digits that are available in commercial software are deemed precise enough not to contribute to the uncertainty of the area. The proof of this is left up to the reader.

The diameter throat of the nozzle will change with temperature in accordance with Equation B2.3

$$D_{Nxt2} = D_{Nx} * \left((t_2 - t_1) * \alpha + 1\right) \qquad \text{B2.3}$$

where α is the thermal expansion coefficient for aluminum $22\text{x}10^{-6}$ m/(m-K) [$12.3\text{x}10^{-6}$ in/in-°F]

Table B2-2. D_{nxt2} Computations

Nozzle Number	Nozzle Throat Diameter	D_{nxt2}	
		SI	I-P
		m	in
1	0.1524 m (6 in.)	0.15235	5.9991
2	0.1016 m (4 in.)	0.10159	3.9994
3	0.0762 m (3 in.)	0.076189	2.9996
4	0.0508 m (2 in.)	0.050793	1.9997

Note: For simplification of this example, this correction will not be carried through the example as it would require additional uncertainty calculations for the temperature measurements and thermal expansion coefficients. One can see that for the 0.1524 m (6 in.) throat diameter nozzle the error in diameter is on the same order as the measurement error in the diameter for this relatively small temperature change. For the small nozzle, the change in diameter is approximately one order of magnitude smaller than the measurement error in the diameter.

Evaluating the derivative of Equation B2.1. For example,

$$\frac{\partial A_1}{\partial D_{N1}} = \frac{\pi D_{N1}}{2} = 0.23939 \text{ m } (9.4248 \text{ in.}) \qquad \text{B2.4}$$

Table B2-3. Result of $\frac{\partial A_x}{\partial D_{Nx}}$ Computations

Nozzle Number	Nozzle Throat Diameter	$\frac{\partial A_x}{\partial D_{Nx}}$	
		SI	**I-P**
		m	**in.**
1	0.1524 m (6 in.)	0.23939	9.4348
2	0.1016 m (4 in.)	0.15960	6.2832
3	0.0762 m (3 in.)	0.11970	4.7124
4	0.0508 m (2 in.)	0.079797	3.1416

$$\Delta D_{N1} = \Delta D_{N2} = \Delta D_{N3} = \Delta D_{N4} = \pm\, 0.0000254 \text{ m } (\pm\, 0.001 \text{in.}) \qquad \text{B2.5}$$

Inserting the values into Equation B2.2, yields the results shown in Table B2-4.

Table B2-4. Result of ΔA_x Computations

Nozzle Number	Nozzle Throat Diameter	ΔA_x	
		SI	**I-P**
		m²	**ft²**
1	0.1524 m (6 in.)	$\pm 6.0805 \times 10^{-6}$	$\pm 6.5450 \times 10^{-5}$
2	0.1016 m (4 in.)	$\pm 4.0537 \times 10^{-6}$	$\pm 4.3633 \times 10^{-5}$
3	0.0762 m (3 in.)	$\pm 3.0402 \times 10^{-6}$	$\pm 3.2725 \times 10^{-5}$
4	0.0508 m (2 in.)	$\pm 2.0268 \times 10^{-6}$	$\pm 2.1817 \times 10^{-5}$

B3 – Uncertainty in Conversion Factor of 1097.8 (for I-P only)

The uncertainty in conversion factor 1097.8 (IP only) needs to be evaluated using Equation 9.5.3.13.

$$Q = 1097.8[\sum(CA)]\varepsilon\sqrt{\frac{\Delta p}{\rho_1}} \qquad \text{ft}^3/\text{m (I-P)} \qquad 9.5.3.13$$

The numerical constants and units results in

$$\text{ft}^3/\text{min} = \text{ft}^2\sqrt{\frac{2*(\text{inch of water conventional})}{\text{lb}_\text{m}/\text{ft}^3}} \qquad \text{B3.1}$$

Thus some conversion factors are required to make the units on each side of the equation consistent.

1 inch of water conventional = 25.4 mm of water conventional (Exact conversion based on NIST Guide to the SI).

1 mm of water conventional = 9.80665 Pa (Source BS EN ISO 80000-4:2013).

1 Pa = psia/6894.8.

1 inch of water conventional=25.4 mm of water conventional*(9.80665 Pa/1 mm of water conventional)*(1*psia/6894.8 Pa)=0.036127 psia.

1 psia = 1 lb_f/ in^2 *(12 inch/1ft)^2=144 $\text{lb}_\text{f}/\text{ft}^2$.

1 inch of water conventional=0.036127 psia *144 $\text{lb}_\text{f}/\text{ft}^2$- psia=5.2023 $\text{lb}_\text{f}/\text{ft}^2$.

$$\text{ft}^3/\text{min} = \text{ft}^2\sqrt{\frac{2*5.2023\ \text{lb}_\text{f}/\text{ft}^2}{\text{lb}_\text{m}/\text{ft}^3}} \qquad \text{B3.2}$$

g_c = 9.80665 m/s^2 (Exact based on NIST Guide to the SI).

1 ft = 0.3048 m (Exact based on NIST Guide to the SI).

g_c = 9.80665 m/s^2*1 ft/0.3048 m = 32.174 ft/s^2.
g_c = 32.174 (lb_m·ft)/(lb_f·s^2).

60 sec = 1 min

$$\mathrm{ft^3/min} = \mathrm{ft^2}\sqrt{\frac{2*5.2023\ \mathrm{lb_f}\frac{\mathrm{lb_f}}{\mathrm{ft^2}}*32.174\frac{\mathrm{lb_m\cdot ft}}{\mathrm{lb_f\cdot s^2}}*(60\ \mathrm{sec/min})^2}{\mathrm{lb_m/ft^3}}} \qquad \text{B3.3}$$

$$\frac{\mathrm{ft^3}}{\mathrm{min}} = 1097.8\ \mathrm{ft^3/min} \qquad \text{B3.4}$$

The conversion factor error due to rounding in the above 1097.8 calculated result is ±0.0012%. This rounded conversion factor uncertainty is used in Equation B10.2.

B4 – Uncertainty in ε

The uncertainty in the multiple nozzle expansibility factor, ε, needs to be evaluated using Equation 9.3.5.9 after substituting γ=1.4 and β = 0.

$$\varepsilon = \left[r^{\frac{2}{\gamma}} \left(\frac{\gamma}{\gamma-1}\right) \left(\frac{1-r^{\frac{\gamma-1}{\gamma}}}{1-r}\right) \left(\frac{1-\beta^4}{1-\beta^4 r^{\frac{2}{\gamma}}}\right) \right]^{1/2} \qquad \text{(SI \& I-P)} \qquad 9.5.3.9$$

$$\Delta\gamma = \pm\sqrt{\left(\frac{\partial\gamma}{\partial p}\times\Delta p\right)^2 + \left(\frac{\partial\gamma}{\partial t}\times\Delta t\right)^2 + \left(\frac{\partial\gamma}{\partial w}\times\Delta w\right)^2} \qquad \text{(SI \& I-P)} \qquad \text{B4.1}$$

$\frac{\partial\gamma}{\partial p}$ is evaluated numerically using the moist air properties spreadsheet called LibHuAirProp (Reference 1).

$$\left(\frac{\partial\gamma}{\partial p}\right) = 1.8966 * 10^{-5} * \frac{1}{\mathrm{kPa}} \quad \text{(SI)} \qquad \text{B4.2}$$

$$\left(\frac{\partial\gamma}{\partial p}\right) = 0.00013077 * \frac{1}{\mathrm{psia}} \quad \text{(I-P)} \qquad \text{B4.3}$$

For this application (other applications at different altitudes would be different) Δp with respect to p_1=101.325 kPa (14.696 psia) can be assumed to be

Δp= ± 1.4946 kPa

Δp= ±6 in. H_2O=±0.21678 psia

$\frac{\partial\gamma}{\partial t}$ is evaluated numerically with LibHuAirProp .

$$\left(\frac{\partial\gamma}{\partial t}\right) = -3.9996 * \frac{10^{-5}}{{}^{o}\mathrm{C}} \quad \text{(SI)}$$

$$\left(\frac{\partial\gamma}{\partial t}\right) = -2.222 * \frac{10^{-5}}{{}^{o}\mathrm{F}} \quad \text{(I-P)}$$

For this application (other applications, say heating mode of a heat pump would be different), Δt with respect to 22 $^{4}/_{18}$ °C [72 °F] can be assumed to be

$$\Delta t = \pm 6\tfrac{2}{3}\ ^{o}C \qquad \text{B4.4}$$

$$\Delta t = \pm 12\ ^{o}F \qquad \text{B4.5}$$

$\frac{\partial \gamma}{\partial w}$ is evaluated numerically with LibHuAirProp .

$$\left(\frac{\partial \gamma}{\partial w}\right) = -0.135 \text{ (SI and I-P)} \qquad \text{B4.6}$$

For this application (other applications, say heating mode of a heat pump), Δw with respect to dry air can be assumed to be the difference between saturated air at t_l=15 $^{10}/_{18}$ °C (60 °F) and dry air.

$$\Delta w = \pm 0.0111 \text{ (SI \& I-P)} \qquad \text{B4.7}$$

Evaluating Equation B4.1:

$$\Delta\gamma = \pm\sqrt{(1.8966 * 10^{-5} \times 1.4946\,)^2 + \left(-3.9996 * 10^{-5} \times 6\tfrac{2}{3}\right)^2 + (-0.135 \times 0.0111)^2} \qquad \text{(SI)}$$

$$\Delta\gamma = \pm\sqrt{(0.00013077 \times 0.21678)^2 + (-2.222 * 10^{-5} \times 12)^2 + (-0.135 \times 0.0111)^2} \text{ (IP)}$$

$$\Delta\gamma = \pm 0.001522 \qquad \text{(SI \& I-P)} \qquad \text{B4.8}$$

The largest β would be for D_{N1}. Assuming that the diameter of the chamber is 0.9144 m (36"), then

$$\Delta\beta = \pm 0.167 = \pm 0.1524\ /\ 0.9144 \quad \text{(SI)} \qquad \text{B4.9}$$

$$\Delta\beta = \pm 0.167 = \pm 6/36 \quad \text{(IP)} \qquad \text{B4.10}$$

r = absolute pressure ratio (p_2/p_1), dimensionless:

$$r = \frac{p_1 - \Delta P}{p_1} = \frac{101.08}{101.33} \qquad \text{(SI)}$$

$$r = \frac{p_1 - \Delta P}{p_1} = \frac{14.660}{14.696} \qquad \text{(I-P)}$$

$$r = 0.99755 \qquad \text{(SI and I-P)} \qquad \text{B4.11}$$

$$\Delta r = \pm\sqrt{\left(\frac{\partial r}{\partial p_1} \times \Delta p_1\right)^2 + \left(\frac{\partial r}{\partial \Delta P} \times \Delta(\Delta P)\right)^2} \qquad \text{(SI \& IP)} \qquad \text{B4.12}$$

$$\frac{\partial r}{\partial p_1} = \frac{\Delta P}{(p_1)^2} = 1.698 * 10^{-7} \quad \text{(SI)}$$

$$\frac{\partial r}{\partial \Delta P} = \frac{-1}{p_1} = -9.869 * 10^{-3} \quad \text{(SI)}$$

$$\Delta r = \pm\sqrt{(1.698 * 10^{-7} \times 0.0101325\,)^2 + (-9.869 * 10^{-3} \times 0.0017438)^2} \quad \text{(SI)}$$

$$\frac{\partial r}{\partial p_1} = \frac{\Delta P}{(p_1)^2} = 1.171 * 10^{-6} \quad \text{(I-P)}$$
$$\frac{\partial r}{\partial \Delta P} = \frac{-1}{p_1} = -6.805 * 10^{-2} \quad \text{(I-P)}$$

$$\Delta r = \pm\sqrt{(1.171 * 10^{-6} \times 0.00147)^2 + (-6.805 * 10^{-2} \times 0.000253)^2} \quad \text{(I-P)}$$

$$\Delta r = \pm 1.72 * 10^{-5} \quad \text{(SI \& I-P)} \qquad \text{B4.13}$$

From a numerical evaluation of the derivatives of Equation 9.3.5.9

$$\varepsilon = \left[r^{\frac{2}{\gamma}} \left(\frac{\gamma}{\gamma-1}\right) \left(\frac{1-r^{\frac{\gamma-1}{\gamma}}}{1-r}\right) \left(\frac{1-\beta^4}{1-\beta^4 r^{\frac{2}{\gamma}}}\right) \right]^{1/2} \qquad 9.3.5.9$$

$$\frac{\partial \varepsilon}{\partial \gamma} \text{x}\ \Delta\gamma = \pm 7.41 * 10^{-7} \qquad \text{B4.14}$$
$$\frac{\partial \varepsilon}{\partial \beta} \text{x}\ \Delta\beta = \pm 1.4 * 10^{-6} \qquad \text{B4.15}$$

The error in the following simplification due to rounding is $\pm 3.1*10^{-5}$ (turns out this is the dominating error)

$$\varepsilon = 1 - 0.548(1 - r) \qquad 9.3.5.10$$
$$\varepsilon = 1 - 0.548(1 - r) = 1 - 0.548(1 - 0.99755) = 0.99866 \qquad \text{B4.16}$$

$$\frac{\partial \varepsilon}{\partial r} = 0.548 \qquad \text{B4.17}$$

$$\Delta\varepsilon = \pm\sqrt{\left(\frac{\partial \varepsilon}{\partial r} \times \Delta r\right)^2 + \left(\frac{\partial \varepsilon}{\partial \beta} \text{x}\ \Delta\beta\right)^2 + \left(\frac{\partial \varepsilon}{\partial \gamma} \text{x}\ \Delta\gamma\right)^2 + (\text{rounding})^2} \quad \text{(SI \& I-P)} \qquad \text{B4.18}$$

$$\Delta\varepsilon = \pm\sqrt{(0.548 \times 1.73 * 10^{-5})^2 + (1.4 * 10^{-6})^2 + (7.41 * 10^{-7})^2 + (3.1 * 10^{-5})^2}$$

$$\Delta\varepsilon = \pm 3.2456 * 10^{-5} \quad \text{(SI \& IP)} \qquad \text{B4.19}$$

B5 – Uncertainty in Density (ρ_1)

To evaluate the uncertainty in C (nozzle discharge coefficient for a multi-nozzle chamber), the uncertainty in ρ_1 needs to be evaluated.

ρ_1 = 1.2156 kg/m^3 (0.075888 lb$_m$/ft^3) as calculated from LibHuAirProp B5.1

$$\Delta\rho_1 = \pm\sqrt{\left(\frac{\partial \rho_1}{\partial t_1} \times \Delta t1\right)^2 + \left(\frac{\partial \rho_1}{\partial W} \times \Delta W\right)^2 + \left(\frac{\partial \rho_1}{\partial p_1} \times \Delta p_1\right)^2 + (\Delta\rho_1 \text{ eqn uncertainty})^2} \qquad \text{B5.2}$$

$$\rho_1 = \rho_{1DA} + \rho_{1W} \qquad \text{B5.3}$$

The equations of LibHuAirProp can be seen in ASHRAE RP-1485's Final Report (Reference 1). The density of air comes from Lemmon, E.W.; Jacobsen, R.T.; Penoncello, S.G.; Friend, D.G.: Thermodynamic Properties of Air and Mixtures of Nitrogen, Argon, and Oxygen from 60 to 2000 K at Pressures to 2000 MPa. J. Phys. Chem. Ref. Data 29, 331-385 (2000). This document states "In the range from the solidification point to 873 K at pressures to 70 MPa, the estimated uncertainty of density values calculated with the equation of state is 0.1%."

The density of water comes from the International Association for the Properties of Water and Steam document number IAPWS-95 which, in Figure 1, states that the uncertainty in water vapor density is 0.001% (or even over a tight range 0.0001%).

Thus a total estimate of uncertainty in the moist air density can be 0.1%.

$$\Delta\rho_1 \text{ eqn uncertainty} = \pm\frac{0.1}{100} * 1.2156 = \pm 1.2156 * 10^{-3}\ \text{kg/m}^3 \qquad \text{B5.4}$$

$$\Delta\rho_1 \text{ eqn uncertainty} = \pm\frac{0.1}{100} * 0.075888 = \pm 7.5888 * 10^{-5}\ \text{lbm/ft}^3 \qquad \text{B5.5}$$

$$W = 0.010462 \text{ as calculated by LibHuAirProp} \qquad \text{B5.6}$$

$\Delta W = \frac{1}{100} * 0.010462 = 0.00010462$ based on Annex C of ASHRAE 41.6-2014 and taking a middle uncertainty of 1% between the two points offered in the last paragraph. For a detailed uncertainty, not just an example as offered in this Annex B, one would need to calculate ΔW based on the example in Annex C of ASHRAE 41.6-2014 of the actual operating or worse case conditions.

For the purpose of coming up with the quantities $\frac{\partial\rho_1}{\partial t_1}$, $\frac{\partial\rho_1}{\partial W}$, and $\frac{\partial\rho_1}{\partial p_1}$, equation 28 of 2013 ASHRAE Handbook – Fundamentals Chapter 36 can be used as a close approximation.

In SI units,

$$\frac{1}{\rho_1} = 0.28704 * (\,t_1 + 273.15) * (1 + 1.6079 * W)/\,p_1$$

$$\rho_1 = \frac{p_1}{0.28704*(\,t_1+273.15)*(1+1.6079*W)}$$

$$\frac{\partial\rho_1}{\partial t_1} = -\frac{p_1}{0.28704*(t_1+273.15)^2*(1+1.6079*W)} = -0.004165$$

$$\frac{\partial\rho_1}{\partial W} = -\frac{1.6079*p_1}{0.28704*(t_1+273.15)*(1+1.6079*W)^2} = -1.9014$$

$$\frac{\partial\rho_1}{\partial p_1} = \frac{1}{0.28704*(\,t_1+273.15)*(1+1.607*W)} = 0.011867$$

In I-P units,

$$\frac{1}{\rho_1} = 0.37049 * (\,t_1 + 459.67) * (1 + 1.6079 * W)/\,p_1$$

$$\rho_1 = \frac{p_1}{0.37049*(\,t_1+459.67)*(1+1.6079*W)}$$

$$\frac{\partial\rho_1}{\partial t_1} = -\frac{p_1}{0.37049*(t_1+459.67)^2*(1+1.6079*W)} = -0.00014445$$

$$\frac{\partial\rho_1}{\partial W} = -\frac{1.6079*p_1}{0.37049*(t_1+459.67)*(1+1.6079*W)^2} = -0.1187$$

$$\frac{\partial\rho_1}{\partial p_1} = \frac{1}{0.37049*(\,t_1+459.67)*(1+1.6079*W)} = 0.005108$$

Substituting the above values into Equation B5.2 results in:

$$\Delta\rho_1 = \pm 0.0012390 \text{ kg/m}^3 \text{ (SI)} \qquad \text{B5.7}$$

$$\Delta\rho_1 = \pm 7.7349 * 10^{-5} \text{ lb}_m/\text{ft}^3 \text{ (I-P)} \qquad \text{B5.8}$$

B6 – Uncertainty in Viscosity

$\mu_1 = 1.7899*10^{-5}$ Ns/m^2 or Pa*s ($1.2028*10^{-5}$ lb$_m$/ft-s) as calculated by LibHuAirProp

The equation sources of LibHuAirProp can be seen in the User's Guide that comes with the software. The viscosity of air comes from Lemmon, E.W.; Jacobsen, R.T.: Viscosity and Thermal Conductivity Equations for Nitrogen, Oxygen, Argon, and Air. Int. J. Thermophys. 25, 21-69 (2004) for the dry air with an uncertainty of 1% and IAPWS. Release on the International Association for the Properties of Water and Steam Formulation 2008 for the Viscosity of Ordinary Water Substance. (2008), available from www.iapws.org for the viscosity of water with an uncertainty of 0.17%."

A detailed comparison could be accomplished using mixing rules to determine the total uncertainty of the moist air viscosity, though given that moist air is mostly air, the uncertainty of the air viscosity is dominating, and there is some uncertainty in the mixing rules, a conservative approach of the following is used:

$$\Delta\mu 1 \text{ eqn uncertainty} = \pm\sqrt{(1\%)^2 + (0.17\%)^2} = 1.01\%$$

$$\Delta\mu_1 \text{ eqn uncertainty} = \pm\sqrt{(1\%)^2 + (0.17\%)^2} = \frac{1.01}{100} * 1.7899 * 10^{-5} = 1.808 * 10^{-7} \text{ Pa} * \text{s (SI)}$$

$$\Delta\mu_1 \text{ eqn uncertainty} = \pm\sqrt{(1\%)^2 + (0.17\%)^2} = \frac{1.01}{100} * 1.2028 * 10^{-5} = 1.215 * 10^{-7} \text{ lb}_m/(\text{ft} * \text{s}) \text{ (I-P)}$$

$$\Delta\mu_1 = \pm\sqrt{\left(\frac{\partial\mu_1}{\partial t_1} \times \Delta t1\right)^2 + \left(\frac{\partial\mu_1}{\partial W} \times \Delta W\right)^2 + \left(\frac{\partial\mu_1}{\partial p_1} \times \Delta p_1\right)^2 + (\Delta\mu 1 \text{ eqn uncertainty})^2} \qquad \text{B6.1}$$

$\frac{\partial\mu_1}{\partial t_1}$ is evaluated numerically with LibHuAirProp .

$$\frac{\partial\mu_1}{\partial t_1} = 4.720*10^{-11} \text{ Pa*s/}^{\circ}\text{C}$$

$$\frac{\partial\mu_1}{\partial t_1} = 1.762*10^{-11} \text{ lb}_m\text{/ft-s-}^{\circ}\text{F}$$

$\frac{\partial\mu_1}{\partial W}$ is evaluated numerically with LibHuAirProp.

$$\frac{\partial\mu_1}{\partial W} = -8.255*10^{-9} \text{ Pa*s}$$

$$\frac{\partial \mu_1}{\partial W} = -5.547*10^{-9}\ lb_m/ft\text{-}s$$

$\frac{\partial \mu_1}{\partial p_1}$ is evaluated numerically with LibHuAirProp.

$$\frac{\partial \mu_1}{\partial p_1} = 1.132*10^{-16}\ s$$

$$\frac{\partial \mu_1}{\partial p_1} = 5.248*10^{-13}\ lb_m/ft\text{-}s\text{-}psia$$

Substituting values into Equation B6.1 results in:

$$\Delta\mu_1 = \pm 1.808 * 10^{-7} \qquad Pa * s \qquad \text{B6.2}$$

$$\Delta\mu_1 = \pm 1.215*10^{-7}\ lb_m/ft\text{-}s \qquad \text{B6.3}$$

B7 – Uncertainty in Re_x and V_x

$$Re_{dx} = \frac{\rho_1 V_x d_x}{\mu_1} \qquad \text{(SI \& I-P)} \qquad 9.3.5.8$$

where

ρ_1= nozzle inlet air density, kg/m^3 (lb$_m$/ft^3)

V_x =nozzle throat average air velocity, m/s (ft/s)

d_x =nozzle throat diameter, m (ft)

μ_1 =nozzle inlet dynamic viscosity, Ns/m^2 (lb$_m$/s-ft)

Table B7-1. Reynolds Number Computations

Nozzle Number	Nozzle Throat Diameter	Re_{dx}	
		SI	**I-P**
		dimensionless	dimensionless
1	0.1524 m (6 in.)	2.0586 x 10 ^{5}	2.0586 x 10 ^{5}
2	0.1016 m (4 in.)	1.3679 x 10 ^{5}	1.3679 x 10 ^{5}
3	0.0762 m (3 in.)	1.0232 x 10 ^{5}	1.0232 x 10 ^{5}
4	0.0508 m (2 in.)	6.7913 x 10 ^{4}	6.7913 x 10 ^{4}

$$\frac{\partial C_1}{\partial Re_{d1}} = \frac{3.503}{Re_{d1}^{\frac{3}{2}}} - \frac{134.6}{Re_{d1}^{2}} \quad \text{(SI \& I-P)} \qquad B7.1$$

Table B7-2. Results of $\frac{\partial C_x}{\partial Re_{dx}}$ Computations

Nozzle Number	Nozzle Throat Diameter	$\frac{\partial C_x}{\partial Re_{dx}}$	
		SI	**I-P**
		dimensionless	dimensionless
1	0.1524 m (6 in.)	3.4329 x 10^{-8}	3.4329 x 10^{-8}
2	0.1016 m (4 in.)	6.0244 x 10^{-8}	6.0244 x 10^{-8}
3	0.0762 m (3 in.)	9.4171 x 10^{-8}	9.4171 x 10^{-8}
4	0.0508 m (2 in.)	1.9875 x 10^{-8}	1.9875 x 10^{-8}

$$\Delta Re_{dx} = \pm\sqrt{\left(\frac{\partial Re_{dx}}{\partial \rho_1} \times \Delta\rho_1\right)^2 + \left(\frac{\partial Re_{dx}}{\partial V_x} \times \Delta V_x\right)^2 + \left(\frac{\partial Re_{dx}}{\partial d_x} \times \Delta d_x\right)^2 + \left(\frac{\partial Re_{dx}}{\partial \mu_1} \times \Delta\mu_1\right)^2} \qquad B7.2$$

$$\frac{\partial Re_{dx}}{\partial \rho_1} = \frac{V_x d_x}{\mu_1} \quad \text{(SI \& I-P)} \qquad B7.3$$

Table B7-3. Results of $\frac{\partial Re_{dx}}{\partial \rho_x}$ Computations

Nozzle Number	Nozzle Throat Diameter	$\frac{\partial Re_{dx}}{\partial \rho_x}$	
		SI	**I-P**
		m^3/kg	ft^3/lb_m
1	0.1524 m (6 in.)	1.6934×10^5	2.7126×10^6
2	0.1016 m (4 in.)	1.1253×10^5	1.8026×10^6
3	0.0762 m (3 in.)	8.4172×10^4	1.3483×10^6
4	0.0508 m (2 in.)	5.5867×10^4	8.9490×10^5

$$\frac{\partial Re_{dx}}{\partial d_x} = \frac{\rho_1 V_x}{\mu_1} \quad \text{(SI \& I-P)} \qquad \text{B7.4}$$

Table B7-4. Results of $\frac{\partial Re_{dx}}{\partial d_x}$ Computations

Nozzle Number	Nozzle Throat Diameter	$\frac{\partial Re_{dx}}{\partial d_x}$	
		SI	**I-P**
		1/m	**1/ft**
1	0.1524 m (6 in.)	1.3508×10^6	4.1171×10^5
2	0.1016 m (4 in.)	1.3464×10^6	4.1038×10^5
3	0.0762 m (3 in.)	1.3428×10^6	4.0928×10^5
4	0.0508 m (2 in.)	1.3369×10^6	4.0748×10^5

$$\frac{\partial Re_{dx}}{\partial \mu_1} = \frac{-d_x \rho_1 V_x}{\mu_1^2} \quad \text{(SI \& I-P)} \qquad \text{B7.5}$$

Table B7-5. Results of $\frac{\partial Re_{dx}}{\partial \mu_1}$ Computations

Nozzle Number	Nozzle Throat Diameter	$\frac{\partial Re_{dx}}{\partial \mu_1}$	
		SI	**I-P**
		m^2/Ns	$ft\text{-}s/lb_m$
1	0.1524 m (6 in.)	-1.1501×10^{10}	-1.7115×10^{10}
2	0.1016 m (4 in.)	-7.6424×10^{9}	-1.1373×10^{10}
3	0.0762 m (3 in.)	-5.7165×10^{9}	-8.5070×10^{9}
4	0.0508 m (2 in.)	-3.7942×10^{9}	-5.6463×10^{9}

$$\frac{\partial Re_{dx}}{\partial V_x} = \frac{\rho_1 d_x}{\mu_1} \quad \text{(SI \& I-P)} \qquad \text{B7.6}$$

Table B7-6. Results $\frac{\partial Re_{dx}}{\partial V_x}$ Computations

Nozzle Number	Nozzle Throat Diameter	$\frac{\partial Re_{dx}}{\partial V_x}$	
		SI	**I-P**
		s/m	**s/ft**
1	0.1524 m (6 in.)	10350	3174.7
2	0.1016 m (4 in.)	6900.1	2103.1
3	0.0762 m (3 in.)	5175.1	1577.4
4	0.0508 m (2 in.)	3450.0	1051.6

V_x =nozzle throat average air velocity, m/s (ft/s) of nozzle x B7.7

In SI units,

$$V_x = \frac{Q_x}{A_x} = C_x \varepsilon \sqrt{\frac{2\Delta p}{\rho_1}} = \left(0.99855 - \left[\frac{7.006}{\sqrt{Re_{dx}}}\right] + \left[\frac{134.6}{Re_{dx}}\right]\right) * \varepsilon \sqrt{\frac{2\Delta p}{\rho_1}} \quad \text{m/s} \qquad \text{B7.8}$$

In I-P units,

$$V_x = \frac{Q_x}{A_x} = \frac{1097.8}{60} * C_x \varepsilon \sqrt{\frac{\Delta p}{\rho_1}} = 1097.8/60\left(0.99855 - \left[\frac{7.006}{\sqrt{Re_{dx}}}\right] + \left[\frac{134.6}{Re_{dx}}\right]\right) * \varepsilon \sqrt{\frac{\Delta p}{\rho_1}} \quad \text{ft/s} \qquad \text{B7.9}$$

The above equation for V_x is circular and of course requires iteration. Note that Section 9.3.5.4.5 recommends iteration until C matches the previous discharge coefficient within 0.5%. Note this could become a dominating error.

In both SI and I-P units,

$$\Delta V_x = \pm\sqrt{\left(\frac{\partial V_x}{\partial Re_{dx}} \times \Delta Re_{dx}\right)^2 + \left(\frac{\partial V_x}{\partial \varepsilon} \text{ x } \Delta\varepsilon\right)^2 + \left(\frac{\partial V_x}{\partial \Delta p} \text{ x } \Delta(\Delta p)\right)^2 + \left(\frac{\partial V_x}{\partial \rho_1} \text{ x } \Delta\rho_1\right)^2} \quad \text{B7.10}$$

$$\frac{\partial V_x}{\partial Re_{dx}} = \varepsilon\sqrt{\frac{2\Delta p}{\rho_1}} * \left(\frac{3.503}{Re_{dx}^{\frac{3}{2}}} - \frac{134.6}{Re_{dx}^2}\right) \quad \text{(SI)} \quad \text{B7.11}$$

$$\frac{\partial V_x}{\partial Re_{dx}} = 1097.8/60 * \varepsilon\sqrt{\frac{\Delta p}{\rho_1}} * \left(\frac{3.503}{Re_{dx}^{\frac{3}{2}}} - \frac{134.6}{Re_{dx}^2}\right) \quad \text{(IP)} \quad \text{B7.12}$$

Table B7-7. Results of $\frac{\partial V_x}{\partial Re_{dx}}$ Computations

Nozzle Number	**Nozzle Throat Diameter**	$\frac{\partial V_x}{\partial Re_{dx}}$	
		SI	**I-P**
		m/s	**ft/s**
1	0.1524 m (6 in.)	6.9405×10^{-7}	2.2770×10^{-6}
2	0.1016 m (4 in.)	1.2544×10^{-6}	4.1153×10^{-6}
3	0.0762 m (3 in.)	1.9039×10^{-6}	6.2462×10^{-6}
4	0.0508 m (2 in.)	3.4116×10^{-6}	1.1196×10^{-6}

$$\frac{\partial V_x}{\partial \varepsilon} = \sqrt{\frac{2\Delta p}{\rho_1}} * \left(0.99855 - \left[\frac{7.006}{\sqrt{Re_{dx}}}\right] + \left[\frac{134.6}{Re_{dx}}\right]\right) \quad \text{(SI)} \quad \text{B7.13}$$

$$\frac{\partial V_x}{\partial \varepsilon} = 1097.8/60 * \sqrt{\frac{\Delta p}{\rho_1}} * \left(0.99855 - \left[\frac{7.006}{\sqrt{Re_{dx}}}\right] + \left[\frac{134.6}{Re_{dx}}\right]\right) \quad \text{(I-P)} \quad \text{B7.14}$$

Table B7-8. Results of $\frac{\partial V_x}{\partial \varepsilon}$ Computations

Nozzle Number	Nozzle Throat Diameter	$\frac{\partial V_x}{\partial \varepsilon}$	
		SI	**I-P**
		m/s	**ft/s**
1	0.1524 m (6 in.)	6.9405×10^{-7}	2.2770×10^{-6}
2	0.1016 m (4 in.)	1.2544×10^{-6}	4.1153×10^{-6}
3	0.0762 m (3 in.)	1.9039×10^{-6}	6.2462×10^{-6}
4	0.0508 m (2 in.)	3.4116×10^{-6}	1.1193×10^{-5}

$$\frac{\partial V_x}{\partial \Delta p} = \frac{\varepsilon * \sqrt{2}\left(0.99855 - \left[\frac{7.006}{\sqrt{Re_{dx}}}\right] + \left[\frac{134.6}{Re_{dx}}\right]\right)}{\sqrt{\Delta p} * 2 * \sqrt{\rho_1}} \quad \text{(SI)} \qquad \text{B7.15}$$

$$\frac{\partial V_x}{\partial \Delta p} = \frac{1097.8/(60*2) * \varepsilon * \left(0.99855 - \left[\frac{7.006}{\sqrt{Re_{dx}}}\right] + \left[\frac{134.6}{Re_{dx}}\right]\right)}{\sqrt{\Delta p} * \sqrt{\rho_1}} \quad \text{(I-P)} \qquad \text{B7.16}$$

Table B7-9. Results of $\frac{\partial V_x}{\partial \Delta p}$ Computations

Nozzle Number	Nozzle Throat Diameter	$\frac{\partial V_x}{\partial \Delta p}$	
		SI	**I-P**
		m^2-s/kg	**ft/(s-in. H_2O)**
1	0.1524 m (6 in.)	0.039921	32.626
2	0.1016 m (4 in.)	0.039792	32.521
3	0.0762 m (3 in.)	0.039686	32.433
4	0.0508 m (2 in.)	0.039511	32.290

$$\frac{\partial V_x}{\partial \rho_1} = \frac{\varepsilon \Delta p * \left(0.99855 - \left[\frac{7.006}{\sqrt{Re_{dx}}}\right] + \left[\frac{134.6}{Re_{dx}}\right]\right)}{\sqrt{\frac{2\Delta p}{\rho_1} * (\rho_1)^2}} \quad \text{(SI)} \qquad \text{B7.17}$$

$$\frac{\partial V_x}{\partial \rho_1} = -1097.8/60 * \frac{\varepsilon \sqrt{\Delta p} * \left(0.99855 - \left[\frac{7.006}{\sqrt{Re_{dx}}}\right] + \left[\frac{134.6}{Re_{dx}}\right]\right)}{2 * (\rho_1)^{1.5}} \quad \text{(I-P)} \qquad \text{B7.18}$$

Table B7-10. Result of $\frac{\partial V_x}{\partial \rho_1}$ Computations

Nozzle Number	Nozzle Throat Diameter	$\frac{\partial V_x}{\partial \rho_1}$	
		SI	**I-P**
		m^4(kg-s)	**ft^4(lb_m-s)**
1	0.1524 m (6 in.)	8.1807	429.92
2	0.1016 m (4 in.)	8.1544	428.53
3	0.0762 m (3 in.)	8.1325	427.38
4	0.0508 m (2 in.)	8.0966	425.50

Note: For the remainder of Section B7, the focus will be on Nozzle 1 in I-P units to illustrate the calculations required. The calculations for Nozzle 1 in SI units the other nozzles in both SI and I-P units were performed but the details are not included here.

Substituting results into Equation B7.10 for Nozzle 1 in I-P units:

$$\Delta V_1 = \pm\sqrt{(2.2770 * 10^{-6} \times \Delta Re_{d1})^2 + 5.3268 * 10^{-2}} \qquad \text{B7.19}$$

Substituting results into Equation B7.2 for Nozzle 1 in I-P units:

$$\Delta Re_{d1} = \pm\sqrt{(3154.7 \times \Delta V_1)^2 + (4.3677x10^6} \qquad \text{B7.20}$$

By solving the two equations, B7.19 and B7.20, for the two unknowns leads to the results shown in Equations B7.21 and B7.22 for Nozzle 1 in IP units:

$$\Delta Re_{d1} = \pm 2213.2 \qquad \text{B7.21}$$

$$\Delta V_1 = \pm 0.23085 \text{ ft/s} \qquad \text{B7.22}$$

Table B7-11 shows the comparable results for all four of the nozzles in both SI and I-P units.

Table B7-11. Results of ΔRe_{dx} and ΔV_x Computations

Nozzle Number	Nozzle Throat Diameter	ΔRe_{dx}	ΔV_x	
		SI and I-P	**SI**	**I-P**
		dimensionless	**m/s**	ft/s
1	0.1524 m (6 in.)	2213.1	±0.070366	±0.23065
2	0.1016 m (4 in.)	1470.8	±0.070146	±0.22773
3	0.0762 m (3 in.)	1100.4	±0.069967	±0.22715
4	0.0508 m (2 in.)	730.83	±0.069671	±0.22619

B8 – Uncertainty in C

The uncertainty in C (nozzle discharge coefficient for a multiple nozzle chamber) needs to be evaluated.

$$C_x = 0.99855 - \left[\frac{7.006}{\sqrt{Re_d}}\right] + \left[\frac{134.6}{Re_d}\right] \qquad 9.5.3.11$$

Table B8-1. Nozzle Discharge Coefficients

Nozzle Number	Nozzle Throat Diameter	C_x
		SI and I-P
		dimensionless
1	0.1524 m (6 in.)	0.98376
2	0.1016 m (4 in.)	0.98059
3	0.0762 m (3 in.)	0.97796
4	0.0508 m (2 in.)	0.97365

$$\Delta C_x = \pm\sqrt{\left(\frac{\partial C_x}{\partial Re_{dx}} \times \Delta Re_{dx}\right)^2 + (\Delta C\ \text{Eqn. Uncertainty})^2 + (\Delta C\ \text{convergence})^2} \qquad B8.1$$

ΔC convergence $= 0.5\%$, though a stricter limit could be used and credit taken for it.

The empirically-derived nozzle discharge coefficient corrects the theoretical flow equation to the actual flow. "Flow Nozzles with Zero Beta Ratio," by Hans J. Leutheusser published in the Transactions of ASME September 1964 provides a derivation of C purely based on fundamental equations for nozzles with a beta = 0 over a small Re range (10^3<Re<10^6).

$$C=1-6.528/Re^{0.5} \qquad \text{B8.2}$$

Using this C and comparing to the C* ε of this standard, the largest difference is found on the largest nozzle, which also is outside the Re range (Re=$2*10^6$). This difference is on the order of 0.3%, and, as such, a conservative 0.35% uncertainty will be prescribed.

$$\Delta C\ \text{Eqn. Uncertainty} = 0.35\% \qquad \text{B8.3}$$

$$\frac{\partial C_x}{\partial Re_{dx}} = \frac{3.503}{Re_{dx}^{\frac{3}{2}}} - \frac{134.6}{Re_{dx}^2} \qquad \text{B8.4}$$

Table B8-1. Results of ΔC_x Computations

Nozzle Number	Nozzle Throat Diameter	ΔC_x SI and I-P dimensionless
1	0.1524 m (6 in.)	±0.006005
2	0.1016 m (4 in.)	±0.006005
3	0.0762 m (3 in.)	±0.006005
4	0.0508 m (2 in.)	±0.003004

Note: $\Delta C_x = \pm 0.00348$ if the convergence criterion for C is changed to 0.05% from 0.5% which may require one or two more iterations.

B9 – Uncertainty in $\sum(CA)$

$$\sum(CA) = C_1 * A_1 + C_2 * A_2 + C_3 * A_3 + C_4 * A_4 \quad \text{(SI \& I-P)} \qquad \text{B9.1}$$

$$\sum(CA) = 0.032329\ m^2 \quad \text{(SI)} \qquad \text{B9.2}$$

$$\sum(CA) = 0.34798\ ft^2 \quad \text{(I-P)} \qquad \text{B9.3}$$

$$\Delta \sum(CA) = \pm\sqrt{\sum_{i=1}^{4}\left(\frac{\partial \sum(CA)}{\partial C_i} \times \Delta C_i\right)^2} \quad \text{(SI and I-P)} \qquad \text{B9.4}$$

$$\frac{\partial \sum(CA)}{\partial C_x} = A_x \quad \text{(SI and I-P)} \qquad \text{B9.5}$$

$$\frac{\partial \sum(\mathrm{CA})}{\partial \mathrm{A_x}} = \mathrm{C_x} \quad \text{(SI and I-P)} \qquad \text{B9.6}$$

Plugging the known values into Equation B9.4 leads to the results in SI units in Equation B9.7 and in I-P units in B9.8

$$\Delta \sum(\mathrm{CA}) = \pm 0.00012382\ \mathrm{m^2} \qquad \text{(SI)} \qquad \text{B9.7}$$

Note: $\Delta \sum(\mathrm{CA}) = \pm 0.00007203\ \mathrm{m^2}$ if the convergence criterion for C is changed to 0.05% from 0.5% which may require one or two more iterations.

$$\Delta \sum(CA) = \pm 0.0013328\ \mathrm{ft^2} \qquad \text{(I-P)} \qquad \text{B9.8}$$

Note: $\Delta \sum(CA) = \pm 0.00077536\ \mathrm{ft^2}$ if the convergence criterion for C is changed to 0.05% from 0.5% which may require one or two more iterations.

B.10 – Uncertainty in Q

The uncertainty in Q (volumetric duct airflow rate) needs to be evaluated.

$$Q = [\sum(CA)]\varepsilon\sqrt{\frac{2\Delta p}{\rho_1}}\ \mathrm{m^3/s} \qquad \text{(SI)} \qquad 9.3.5.15$$

$$Q = 1097.8[\sum(CA)]\varepsilon\sqrt{\frac{\Delta p}{\rho_1}}\ \mathrm{ft^3/min} \qquad \text{(I-P)} \qquad 9.3.5.16$$

In SI units,

$$\Delta Q = \pm\sqrt{\left(\frac{\partial Q}{\partial \sum(CA)} \times \Delta \sum(CA)\right)^2 + \left(\frac{\partial Q}{\partial \varepsilon} x\ \Delta\varepsilon\right)^2 + \left(\frac{\partial Q}{\partial \Delta p} x\ \Delta(\Delta p)\right)^2 + \left(\frac{\partial Q}{\partial \rho_1} x\ \Delta\rho_1\right)^2} \qquad \text{B10.1}$$

In I-P units,

$$\Delta Q = \pm\sqrt{\left(\frac{\partial Q}{\partial \sum(CA)} \times \Delta \sum(CA)\right)^2 + \left(\frac{\partial Q}{\partial \varepsilon} x\ \Delta\varepsilon\right)^2 + \left(\frac{\partial Q}{\partial \Delta p} x\ \Delta(\Delta p)\right)^2 + \left(\frac{\partial Q}{\partial \rho_1} x\ \Delta\rho_1\right)^2 + (Conversion\ Factor)^2} \qquad \text{B10.2}$$

$$\frac{\partial Q}{\partial \sum(CA)} = \varepsilon\sqrt{\frac{2\Delta p}{\rho_1}} = 20.2175 \qquad \text{B10.3}$$

$$\frac{\partial Q}{\partial \sum(CA)} = 1097.8\varepsilon\sqrt{\frac{\Delta p}{\rho_1}} = 3979.72 \qquad \text{B10.4}$$

$$\frac{\partial Q}{\partial \varepsilon} = \sum(CA)\sqrt{\frac{2\Delta p}{\rho_1}} = 0.65448\ \mathrm{m^3/s} \qquad \text{B10.5}$$

$$\frac{\partial Q}{\partial \varepsilon} = 1097.8\sum(CA)\sqrt{\frac{\Delta p}{\rho_1}} = 1386.7\ \mathrm{ft^3/min} \qquad \text{B9.6}$$

$$\frac{\partial Q}{\partial \Delta p} = \frac{\sum(CA)\,\varepsilon}{\rho_1 * \sqrt{\frac{2\Delta p}{\rho_1}}} = 0.001312 \text{ m}^3\text{/s-Pa} \qquad \text{B9.7}$$

$$\frac{\partial Q}{\partial \Delta p} = \frac{1097.8\sum(CA)\,\varepsilon}{2 * \rho_1 * \sqrt{\frac{\Delta p}{\rho_1}}} = 692.435 \text{ ft}^3\text{/(min-in. H}_2\text{O Conventional)} \qquad \text{B9.8}$$

$$\frac{\partial Q}{\partial \rho_1} = \frac{-\sum(CA)\,\varepsilon\,\Delta p}{(\rho_1)^2 * \sqrt{\frac{2\Delta p}{\rho_1}}} = -0.26884 \qquad \text{(SI)} \qquad \text{B9.9}$$

$$\frac{\partial Q}{\partial \rho_1} = \frac{-1097.8\sum(CA)\,\varepsilon\,\Delta p}{2 * (\rho_1)^2 * \sqrt{\frac{\Delta p}{\rho_1}}} = -9124.4 \qquad \text{(I-P)} \qquad \text{B9.10}$$

Substituting values into Equations B10.1 and Equation 9.3.5.12 in SI units results in Equation B10.11 and B10.12, and substituting values into Equations B10.1 and Equation 9.3.5.13 in I-P units results in Equation B10.13 and B10.14.

$$\Delta Q = \pm\, 0.003408 \text{ m}^3\text{/s} \qquad \text{B10.11}$$

Note: $\Delta Q = \pm 0.002732$ m^3/s if the convergence criterion for C is changed to 0.05% from 0.5% which may require one or two more iterations.

$$Q = 0.6536 \text{ m}^3\text{/s} \qquad \text{B10.12}$$

$$\Delta Q = \pm\, 7.2149 \text{ ft}^3\text{/min} \qquad \text{B10.13}$$

Note: $\Delta Q = \pm 5.7893$ ft^3/s if the convergence criterion for C is changed to 0.05% from 0.5% which may require one or two more iterations.

$$Q = 1384.9 \text{ ft}^3\text{/min} \qquad \text{B10.14}$$

Summarizing the results and expressing both the calculated result and its associated uncertainty in a reasonable number of significant figures yields for SI units:

$$Q = 0.6536 \text{ m}^3\text{/s} \pm 0.0034 \text{ m}^3\text{/s} \qquad \text{B10.15}$$

and for IP units:

$$Q = 1385 \text{ ft}^3\text{/min} \pm 7 \text{ ft}^3\text{/min} \qquad \text{B10.16}$$

(This annex is not part of this standard. It is merely informative and does not contain requirements necessary for conformance to the standard. It has not been processed according to

the ANSI requirements for a standard and may contain material that has not been subject to public review or a consensus process. Unresolved objectors on informative material are not offered the right to appeal at ASHRAE or ANSI.)

INFORMATIVE ANNEX C: UNCERTAINTY CALCUATIONS FOR AIR VELOCITY MEASUREMENTS USING A PITOT-STATIC TUBE

The air velocity measured using a Pitot-static tube depends on the separate independent measurements of velocity pressure, atmospheric pressure, dry-bulb temperature, and wet-bulb temperature. The velocity measured using a Pitot-static tube is given in Equation C.1 in SI units and in Equation C1.2 in I-P units.

$$V = \sqrt{\frac{2P_v}{\rho}} \text{ m/s (SI)} \qquad \text{C.1}$$

$$V = 1097.8\sqrt{\frac{P_v}{\rho}} \text{ ft/min (I-P)} \qquad \text{C.2}$$

The density can be determined from equations in RP-1485 that depend upon the atmospheric pressure, the dry-bulb temperature, and the wet-bulb temperature. For this analysis, the parameter values are shown in SI in Table C-1 for SI units and Table C-2 for I-P units. Additionally, the analysis is shown in exact values for IP values with the SI values being approximate.

Parameter	Average	Abs Uncertainty (+/-)	Units
Patm	98.2	0.0220	kPa
Pv	99.6	0.249	Pa
Twb	19.4	0.28	C
Tdb	26.7	0.28	C

Table C-1. Assumed parameter values in SI

Parameter	Average	Abs Uncertainty (+/-)	Units
Patm	29.0	0.0065	In Hg
Pv	0.400	0.001	In H20
Twb	67.0	0.5	F
Tdb	80.0	0.5	F

Table C-2. Assumed parameter values in I-P

Using the parameter values to obtain the density from RP-1485, the following values are calculated:

$$\rho_o = 1.136 \text{ kg/m}^3 \text{ (SI)} \qquad \text{C.3}$$

$$\rho_o = 0.07074 \text{ lb}_m\text{/ft}^3 \text{ (I-P)} \qquad \text{C.4}$$

$$V = \sqrt{\frac{2P_v}{\rho_o}} = 13.24 \text{ m/s (SI)} \qquad \text{C.5}$$

$$V = 1097.8 * \sqrt{\frac{P_v}{\rho_o}} = 2610 \text{ ft/min (I-P)} \qquad \text{C.6}$$

The total uncertainty associated with the air velocity measurement can be determined by Equation C.7.

$$\sigma_{total}{}^2 = \sigma_{T_{db}}{}^2 + \sigma_{T_{wb}}{}^2 + \sigma_{P_{atm}}{}^2 + \sigma_{P_v}{}^2 + \sigma_{\theta}{}^2 \qquad \text{C.7}$$

Each uncertainty can be determined by Equation C.8.

$$\sigma_x{}^2 = \left(\frac{1}{\bar{y}}\frac{\partial y}{\partial x}u_x\right)^2 \qquad \text{C.8}$$

Where u_x is the instrument manufacturer's stated accuracy for the measured quantity under evaluation. When the above equation is solved for each input parameter the calculated uncertainty is 0.1%, which should be expressed as Equation C.9 in SI units and Equation C.10 in I-P units.

$$13.24 \pm 0.02 \text{ m/s (SI)} \qquad \text{C.9}$$

$$2610 \pm 3.5 \text{ ft/min (I-P)} \qquad \text{C.10}$$

Parameter	Absolute Uncertainty $\partial y/\partial x\ u_x$	Relative Uncertainty $1/\bar{y}\ \partial y/\partial x\ u_x$	Contribution
P_{atm}	0.001	0.01%	0.72%
P_v	0.017	0.13%	88.14%
T_{wb}	0.001	0.01%	0.67%
T_{db}	0.006	0.04%	10.46%

Table C-3. Uncertainty associated with each measured parameter for SI

Parameter	Absolute Uncertainty ∂y/∂x u_x	Relative Uncertainty 1/$\bar{y}$ ∂y/∂x u_x	Contribution
P_{atm}	0.295	0.01%	0.72%
P_v	3.262	0.12%	88.14%
T_{wb}	0.285	0.01%	0.67%
T_{db}	1.124	0.04%	10.46%

Table C-4. Uncertainty associated with each measured parameter for IP

It is important to also note that the above analysis is only applicable when the Pitot-static tube is oriented in the airflow. Experimental measurements of the Pitot-static tube in Figure C-1 shows the effect of misalignment on the accuracy of the velocity measurement – this is why there is a ± 10 degree alignment restriction in this standard. Moreover, this dependence is defined by a coefficient of pressure, which is defined by Equation C.11 and plotted in Figure C-1 [See Annex A Section A5 for more detailed information].

$$C_P = \frac{P_V}{\frac{1}{2}\rho V^2} \qquad \text{C.11}$$

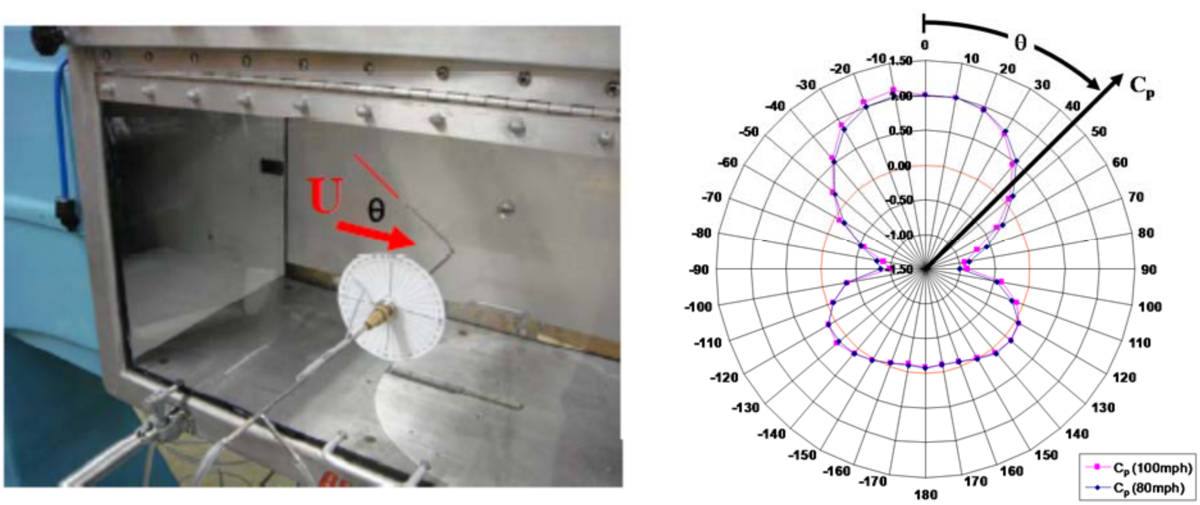

Figure C-1. Experimental Test Set Up (left) to Determine the Dependence of the Angle of Attack on the Coefficient of Pressure (right).

(This annex is not part of this standard. It is merely informative and does not contain requirements necessary for conformance to the standard. It has not been processed according to the ANSI requirements for a standard and may contain material that has not been subject to public review or a consensus process. Unresolved objectors on informative material are not offered the right to appeal at ASHRAE or ANSI.)

INFORMATIVE ANNEX D: SUPPLEMENTARY UNCERTAINTY CALCULATION PROCEDURES

D1. Exact conversion of 1.202 kg/m^3 to lb$_m$/ft^3

D1.1 Exact Conversions. When conversions between different systems of units are made, uncertainty needs to be accounted for if exact conversions are not used. Exact conversions often can be obtained with no added uncertainty as one system of units is often defined as a certain quality of the SI equivalent. NIST Special Publication 1038 – The International System of Units (SI) – Conversion Factors for General Use, is a good source of conversion factors, though note only the conversion factors in bold in this document are exact.

D1.2 Exact conversion of m to ft. The conversion from m to ft can be found on page 8 of NIST Special Publication 1038 and is reproduced below.

$$1 \text{ ft} = 0.3048 \text{ m (exact)} \qquad \text{D1.1}$$

D1.3 Exact conversion of kg to lb$_m$. The conversion from kg to lb$_m$ can be found on page 11 of NIST Special Publication 1038 and is reproduced below.

$$1 \text{ lb}_m = 0.45359237 \text{ kg (exact)} \qquad \text{D1.2}$$

D1.4 Exact conversion of 1.202 kg/m^3 to lb$_m$/ft^3. The conversion from 1.202 kg/m^3 to lb$_m$/ft^{3}can be found by mathematical functions from the conversions in Equations D1.1 and D1.2.

$$1.202 \text{ kg/m}^3 *(1 \text{ lb}_m)/(0.45359237 \text{ kg})*(0.3048 \text{ m})^3/(1 \text{ ft})^3 \qquad \text{D1.3}$$

$$=$$

$$1.202 \text{ lb}_m/\text{ft}^3/(0.45359237)*(0.3048\ )^3 \qquad \text{D1.4}$$

$$=$$

$$0.0750384086125258 \text{ lb}_m\ /\text{ft}^3 \text{ (exact)} \qquad \text{D1.4}$$

D1.5 Approximation of 1.202 kg/m^3 to lb$_m$/ft^3. The conversion from 1.202 kg/m^3 to lb$_m$/ft^{3}can be approximated as 0.075 lb$_m$ /ft^3 with an associated error <+0.00004 lb$_m$ /ft^3. The convention in uncertainty analysis is to lump errors in with all other unknowns and report a ± value. Thus, the conversion from 1.202 kg/m^3 to lb$_m$/ft^{3}can be approximated as 0.075 lb$_m$ /ft^3 with an associated uncertainty due to the approximation during conversion of ±0.00004 lb$_m$ /ft^3.

(This annex is not part of this standard. It is merely informative and does not contain requirements necessary for conformance to the standard. It has not been processed according to the ANSI requirements for a standard and may contain material that has not been subject to public review or a consensus process. Unresolved objectors on informative material are not offered the right to appeal at ASHRAE or ANSI.)

INFORMATIVE ANNEX E: USER INFORMATION

E1. Introduction. The content of this annex is intended to provide advice and commentary to augment the information presented within the body of the standard. Note that the advice and commentary in this annex is not necessarily supported by peer-reviewed references. If this annex contains any information that is contrary to the information presented in the body of the standard, disregard the information in this annex.

E2. Comparison of Airflow Measurements. Table E2.1 provides general information and commentary regarding the airflow measurement methods that are included in this standard.

Table B2.1: Summary of Airflow Measurement Methods

Section	Method	Typical Airflow or Air Velocity Range	Typical Accuracy (percent of reading)	Applications	Comments
9.2	Pitot-static Tube: • Single Pitot-tubes • Pitot-static Tube Traverse • Self-Averaging Arrays • Self-Averaging Probes	4-50 m/s (800-10,000 fpm)	±2% to ±10%	Hand-held instruments used for field measurement; fixed position in laboratories.	Alignment with airstream direction is critical
9.3	Single and Multiple Airflow Nozzles	Throat velocity ≥ 3000 fpm (15 m/s)	±0.5% to ±2%	Widely used for laboratory and field measurements.	No comment
9.4	Thermal Dispersion Array	(10-10,000 fpm)	±1% to ±10%	Often used for inlet measurements. Low velocity capabilities.	Some thermistors are not designed for repeated heating and cooling cycles.
9.5	Vortex Shedding Arrays	No comment	No comment	No comment	No comment

9.6	Capture Hoods	17 - 4250 m^3/h (10 -2500 cfm)	±3%	Measure airflow rates into/out of system air delivery vents and diffusers.	Correction factors may be required as needed by diffuser type.
9.7	Tracer Gas	No comment	No comment	No comment	Used to measure building air change rates and for calibrating other airflow meters.

E3. Comparison of Air Velocity Measurement Methods. Table E3.1 provides general information and commentary regarding the air velocity measurement methods that are included in this standard.

Table E3.1: Summary of Air Velocity Measurement Methods

Section	Air Velocity Measurement Method	Typical Air Velocity Range	Typical Accuracy	Comments
7.2.	Pitot-Static Tube	3-50 m/s (600-10,000 fpm)	±2% to ±5%	Adversely affected by misalignment with the airstream.[A1]
7.3	Thermal Anemometer	0.1-50 m/s (10-10,000 fpm)	±2% to ±10%	Adversely affected by thermal plume at low airflows.
7.4	Rotary Vane Anemometer	0.03-30 m/s (60-6000 fpm)	±2% to ±5%	Adversely affected by turbulence intensity.
7.5	Drag-Force Velocity Meter	0.1-50 m/s (10-10,000 fpm)	±2%	No comment
7.6	Laser Doppler Velocimeter	0.005-50 m/s (1-10,000 fpm)	±1% to 3%	Requires optical access. High cost.

E4. Commentary Regarding Default Steady-State Criteria for Air Velocity and Airflow Measurements. The comments in this section generally apply to both air velocity and volumetric as well as mass airflow rate default steady-state criteria; however, Equations 5.3.1.1 through 5.3.1.3 apply specifically to the air velocity and Equations 5.3.2.1 through 5.3.2.3 apply specifically to airflow default steady-state criteria. Only the steady-state criteria in reference to air velocity measurements will be specifically illustrated here, but the extension of the discussion to steady-state volumetric as well as mass airflow rate is straightforward.

The basic criteria established in Section 5.3.1 indicates that if the test plan in Section 5.1 requires air velocity data points to be recorded at steady-state test conditions but does not specify the steady-state criteria, then the criteria for establishing steady-state test conditions shall be determined according to the procedures given below.

If the test plan in Section 5.1 specifies a target air velocity for the steady state test conditions, V_{target}, then the targeted steady-state conditions shall be established according to Equations 5.3.1.1.

$$\left|\frac{\bar{V}-V_{target}}{V_{target}}\right| \leq 1\% \qquad 5.3.1.1$$

where

V_{target} = target air velocity specified in Section 5.1.
$\bar{V}$ = the arithmetic mean value of the air velocity measurements obtained from Equation 5.3.1.2, m/s (fpm)
n = number of measurement samples. There shall be at least 10 measurement samples as required by Equation 5.3.1.3.

$$\bar{V} = \frac{1}{n}\sum_{i=1}^{n} V_i \qquad 5.3.1.2$$

$$n \geq 10 \qquad 5.3.1.3$$

This is graphically illustrated in Figure E4.1, which shows a sampled velocity signal with random fluctuations.

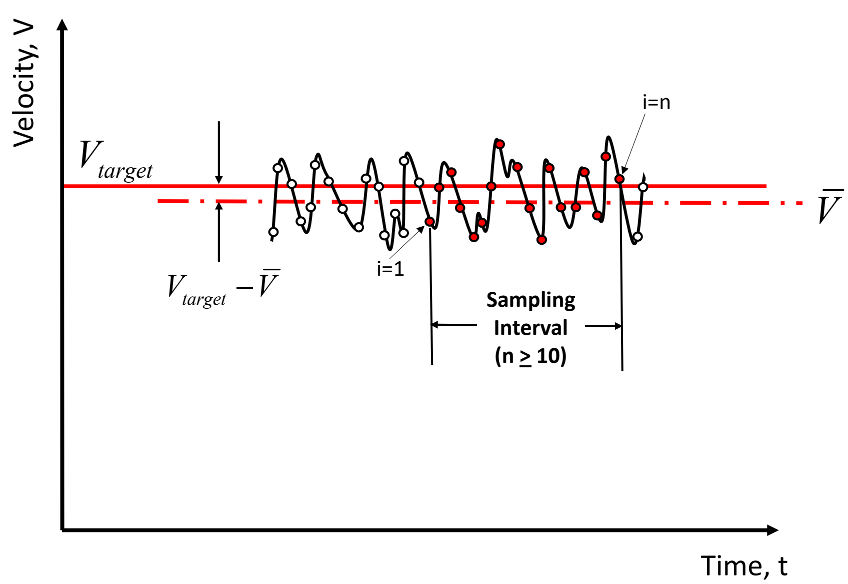

Figure E4.1: Targeted Steady-State Conditions

If no specific target velocity is specified in the test plan, then steady-state conditions shall be established when three or more consecutive values of measured mean velocity, $\bar{V}_1, \bar{V}_2, \bar{V}_3 \ldots$ as determined from

Equation 5.3.1.2, are equal to within 1% of the target velocity. The approach to steady-state conditions is illustrated in Figure E4.2, which shows a measured signal being sampled prior to leveling out of the mean. Note that $\bar{V}_{SS}$ represents the final steady-state sampled mean, such that $\bar{V} = \bar{V}_{SS}$.

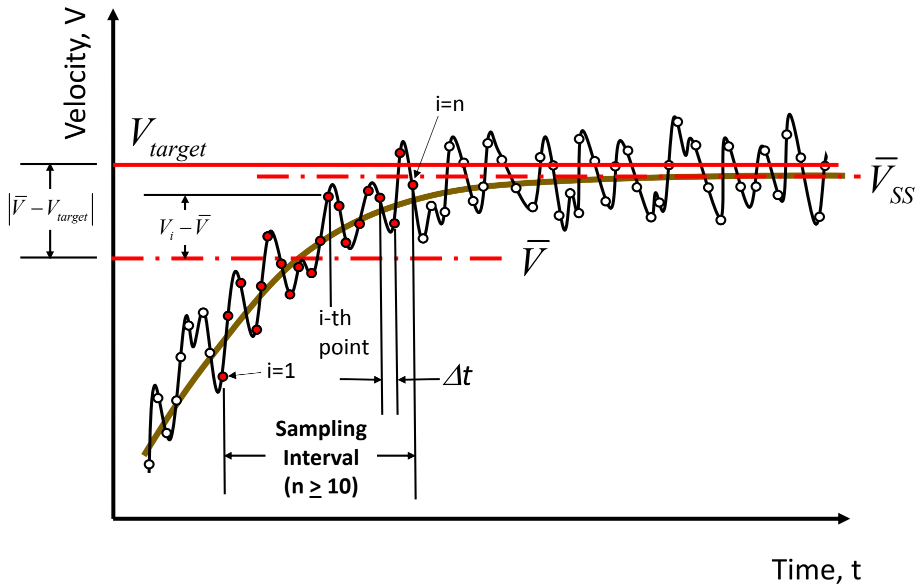

Figure E4.2: The Approach to Steady-State Conditions

There are two important issues that must be addressed in establishing whether steady state conditions have been reached. First, in order for Equation 5.3.1.2 to provide a meaningful representation of the sample statistics (sampled mean velocity), the sampling interval in between each individual signal measurement, Δt, must be sufficiently large such that adjacent measurements are statistically independent. If over-sampling (sampling faster than required) of a quantity is used, the amount of data collected will be large, but it may not provide a representative amount of statistically independent data so as to provide accurate estimates of the statistics. In other words, the "effective sample size," n_{eff}, may be too small and much less than the actual number of samples collected, n. On the other hand, if the observed quantity is under-sampled (slower than the minimum rate), then an excessively large period of time will be required to provide a large enough sample size to achieve accurate statistics.

The second requirement is that the number of samples, n, used to determine the mean and standard deviation of the measured velocity must be selected to be sufficiently large such that the random uncertainties in these quantities are less than the specified tolerance (by the flow measurement standard) used to establish whether the mean is not changing significantly, and that stationary (unchanging statistical) conditions exist during final steady-state conditions. The required minimum sampling time interval can be determined by calculating an autocorrelation of the sampled quantity and observing what sample spacing will reduce the autocorrelation to essentially zero. However, a practical rule of thumb is to sample at a time interval which is no smaller than the period of the lowest observed fluctuation frequency. This will ensure that the actual sample size n is approximately equal to the effective sample size n_{eff}, and all of the data will then contribute to the measured statistics. The procedures outlined in Equations 5.3.1.1 through 5.3.1.3 assume that the effective sample size is sufficiently large so that once steady-state conditions have been reached as shown in Figure E.1, the standard deviation of the measured mean will be less than 1%. The sample size of $n \geq 10$, corresponding to the overall sampling interval shown in Figure E4.2 is specified as a reasonable practical number of independent samples.

E5. Self-Averaging Arrays. Both Pitot-static tube traverse method and self-averaging array devices use the difference between total and static pressures to provide velocity pressure and therefore a means from which velocity can be calculated. Velocity pressure measurement with a Pitot-static tube has been used since 1732. It is reliable, but with limits. It is also the most readily understood method of airflow measurement, making this the most widely taught method in engineering schools.

Self-averaging arrays are not portable but are intended for permanent and fixed installations. They were developed for and have been used in Heating, Ventilation, Air-Conditioning, and Refrigeration (HVAC&R) systems since the 1960s. Their use grew together with that of Variable Air Volume (VAV) air distribution designs.

Also known as a 'self-averaging array,' the Pitot Array can be described as a bifurcated tube with two sets of segregated collection holes, with each set connected to a collection manifold: One set for total pressure and another set for static pressure. The difference between these pressures (ΔP) equals velocity pressure by definition, which can be mathematically converted to air velocity at actual or standard conditions. Although these devices can be equivalent in some laboratory environments or under excellent field conditions (Equation B5.1), they are most often misapplied in conditions unsuited for the technology and thereby producing very poor results. The basic formula for velocity governing both the traverse and the array is:

$$V = K\sqrt{\frac{2\Delta P}{\rho_x}} \quad \text{B5.1}$$

A minimum "straight run" of 10 equivalent duct diameters was required for "acceptable" measurement accuracy. In many cases, a flow-straightening honeycomb was required to minimize the averaging error due to the single pressure outputs from the manifolds, interconnected with the sampling ports.

Self-averaging arrays using a single calibration factor (K-factor) will result in measurement error as the airflow varies to under approximately 5.08 m/s (1,000 FPM). Use of a single K-factor is common for commercial HVAC&R devices. Nonetheless, Pitot arrays can demonstrate accuracies of ±2% (not including errors from the pressure transducer), when compared to laboratory test tunnels having very "flat" velocity profiles with sufficiently high Reynolds numbers (i.e., for V >3.05 m/s (600 ft/min)).

In most cases, the pressure transducer is the greatest source of velocity pressure measurement error, especially at lower flows. Because the relationship of airflow-to-differential pressure is a square root function, the uncertainty of the pressure transducer results in significantly greater "per cent of reading" errors as the airflow is turned down. These uncertainties do not include the contributions from the in-duct device, which may result from turbulence or skewed velocity profiles.

Self-averaging arrays try to equalize non-linear velocity pressure profile from multiple pickup points and use it as an average of total or static pressures across the plane of measurement. Self-averaging arrays averaging errors exceed those of devices using independent sensors, even when the number of pickup points far exceeds the later. As a direct result, the self-averaging array does not have the capabilities or properties of a Pitot traverse or any measurement method or device using individual velocity determinations.

The two methods cannot be equated and any comparison or implied equivalency is superficial. Some have exploited the similarities. Examples include references to the number of arrayed sampling ports (holes) which have been termed 'sensors' or 'sensing points' and that the total number should comply with the quantity and position of velocity determinations in a standardized Pitot traverse. When explained, anyone can understand that they are not comparable. ISO 3966 explains the many sources of Pitot errors, as do the instructions included in ASHRAE Standard 111 and the guidelines of Testing, Adjusting, and Balancing (TAB) national associations.

Pitot traverse and Pitot arrays can be used effectively, but knowledge of their duct position and velocity limitations are needed to ensure optimal performance.

E6. Thermal Anemometers. The thermal (or hot-wire, or hot-film) anemometer consists of a heated resistance temperature device (RTD), thermocouple junction, or thermistor sensor constructed at the end of a probe. It is designed to provide a direct, simple method of determining air velocity at a point in the flow field. The probe is placed into an airstream, and air movement past the electrically heated velocity sensor tends to cool the sensor in proportion to the speed of the airflow. The electronics and sensor are commonly combined into a portable, hand-held device that interprets the sensor signal and provides a direct reading of air velocity in either analog or digital display format. Often, the sensor probe also incorporates an ambient temperature-sensing RTD or thermistor, in which case the indicated air velocity is temperature compensated to standard air density conditions.

Thermal anemometers have long been used in fluid flow research. Research anemometer sensors have been constructed using very fine wires in configurations that allow characterization of fluid flows in one, two, and three dimensions, with sensor/electronics response rates up to several hundred kilohertz. This technology has been incorporated into more ruggedized sensors suitable for measurements in the HVAC&R field, primarily for unidirectional airflow measurement. Omni-directional sensing instruments suitable for thermal comfort studies are also available.

The principal advantages of thermal anemometers are their wide dynamic range and their ability to sense extremely low velocities. Commercially available portable instruments often have a typical accuracy (including repeatability) of 2% to 5% of reading over the entire velocity range. Accuracies of ±2% of reading or better are obtainable from microcontroller (microprocessor)-based thermistor and RTD sensor assemblies, some of which can be factory calibrated to known reference standards (e.g., National Institute of Standards (NIST) air speed tunnels). An integrated microcontroller also allows an array of sensor assemblies to be combined in one duct or opening, providing independently derived velocity and temperature measurements at each point.

Limitations of thermistor-based velocity measuring devices depend on sensor configuration, specific thermistor type used, and the application. At low velocities, thermal anemometers can be significantly affected by their own thermal plumes (from self-heating). Products using this technology can be classified as hand-held instruments or permanently mounted probes and arrays, and as those with analog electronic transmitters and those that are microcontroller-based. Limitations of hand-held and analog electronic thermal anemometers include the following: (1) the unidirectional sensor must be carefully aligned in the airstream (typically to within ±20° rotation) to achieve accurate results; (2) the velocity sensor must be kept clean because contaminant build-up can change the calibration (which may change accuracy performance); and (3) because of the inherent high speed of response of thermal anemometers, measurements in turbulent flows can yield fluctuating velocity measurements.

Electronically controlled time-integrated functions are now available in many digital air velocity meters to help smooth these turbulent flow measurements. Microcontroller-based thermal dispersion devices are typically configured as unidirectional instruments but may have multiple velocity-sensing elements capable of detecting flow direction. These devices can be used to measure a “bleed” air velocity between two spaces or across a fixed orifice. With mathematical conversion, these measured velocities can closely approximate equivalents in differential pressure down to five decimal places (inches of water). They can be used for space pressure control, to identify minute changes in flow direction, or for estimating volumetric flow rates across a fixed orifice by equating to velocity pressure.

In the HVAC&R field, thermal anemometers are suitable for a variety of applications. They are particularly well-suited to the low velocities associated with outside air intake measurement and control, return or relief fan tracking for pressurization in VAV systems, VAV terminal box measurement, unit ventilator and packaged equipment intake measurement, space pressurization for medical isolation, and laboratory fume hood face velocity measurements, typically in the 0.25 m/s (50 fpm) to 0.1 m/s (200 fpm) range. Thermal anemometers can also take multipoint traverse measurements in ventilation ductwork.

E7. Thermal Dispersion Arrays. Energy dissipated from a heated thermistor is directly related to velocity and mass velocity. This is one application of the definition of 'thermal dispersion' based on the known physical relationship between power and a number of variables in a mathematical expression which includes velocity or mass velocity and the temperature difference between a heated source and ambient temperature.

There are several methods used for determining airflow, which is proportional to the rate of heat loss from a temperature dependent resistor device. There are also as many ways as there are manufacturers to use thermal devices as airflow meters. No two are known to be the same and few generalities apply to all. Thermal Dispersion Arrays can only be compared by their measured performance ability and long term reliability.

Some manufacturers use "King's Law" or some form of it to determine the rate of heat-loss to a fluid, which is proportional to flow. One common approach is to measure the power required to keep the device at a constant temperature, which is a measurement of its rate of heat loss. This method requires measuring the voltage across the device at a known resistance. An analog to digital converter is usually required to measure the voltage. Since the power drop across the device is proportional to the square of the voltage, a very precise analog to digital converter is required to measure the voltage to achieve an acceptable power measurement. Since power dissipation is proportional to the square of the voltage, an error in the voltage measurement results in a magnified error in the calculation of the heat loss rate. For example, a voltage measurement error of 5% leads to a 10% error in the heat loss rate measurement calculation.

In another approach, the voltage across the device with a constant current running through it is measured. In this example, the power dissipated can be measured as the product of the voltage and current through the device. However, the temperature of the device, which is an important parameter in determining air flow, varies with the power dissipated and hence the device temperature must be determined independently. Moreover, even this method requires an expensive and precise analog to digital converter.

For industrial applications with higher temperatures and/or corrosive environments, platinum or stainless RTDs are preferred but are not popular in the HVAC&R community. Within HVAC&R comfort applications, thermistors are the sensor of choice because of their relative cost advantage, size, and performance capabilities. For thermistors, the correct industry name is needed for component identification and comparison name which may not be that used in promotional literature by a manufacturer.

The specific thermistor types being used for thermal dispersion airflow measurement devices in the current HVAC market are:

1. Bead-in-Glass (Probe thermistor);
2. several types of Chip thermistors
    a. Chip-in-Glass;

b. Epoxy Coated and
c. Diode Case.

Although originally designed to provide greater interchangeability, consistent temperature performance and mass production for uses such as wall stats and surface mounted to electronics, most thermistors do not have all of the qualities needed for suitability in airflow measurement application. The characteristics that are important for airflow measurement in HVAC&R conditions are: stability or long-term drift characteristics; a design that anticipated its use for self-heat applications; response time or sensitivity to changes; lead conduction; resistance to external sources of corrosion. A deficiency in any of these areas for a sensor used in an airflow measurement assembly would provide a meter that would not perform satisfactorily and/or is likely to fail prematurely.

The nature of the thermistor-sensors' raw output and visible requirement for microprocessor-based electronics led some manufacturers to factory calibration. Some of these designs would not be viable without calibration. Other designs have chosen to leave output adjustment to contractors in the field without any formal calibration process, similar to adjustment methods used by velocity pressure devices. This requires assumptions about the validity of the basic design, sensor, and electronics performance. With proper selection of the components, attention to detail, and a robust design, thermal dispersion devices have demonstrated superior precision, reliability, and a wide performance range for over 30 years.

E8. Airflow Hoods. Flow-measuring hoods are portable instruments designed to measure supply or exhaust airflow through diffusers and grilles in HVAC&R systems. The assembly typically consists of a fabric hood section, a plastic or metal base, an airflow-measuring manifold, ammeter, and handles for carrying and holding the hood in place.

For volumetric airflow measurements, the flow-measuring hood is placed over a diffuser or grille. The fabric hood captures and directs airflow from the outlet or inlet across the flow-sensing manifold in the base of the instrument. The manifold consists of a number of tubes containing upstream and downstream holes in a grid, designed to simultaneously sense and average multiple velocity points across the base of the hood. Air from the upstream holes flows through the tubes past a sensor and then exits through the downstream holes. Sensors used by different manufacturers include swinging vane anemometers, electronic micromanometers, and thermal anemometers. In electronic micromanometers, air does not actually flow through the manifold, but the airtight sensor senses the pressure differential from the upstream to downstream series of holes. The meter on the base of the hood interprets the signal from the sensor and provides a direct reading of volumetric flow in either an analog or digital display format.

As a performance check in the field, the indicated flow of a measuring hood can be compared to a duct traverse flow measurement (using a Pitot-static tube or thermal anemometer). All flow-measuring hoods induce some back pressure on the air-handling system because the hood restricts flow out of the diffuser. This added resistance alters the true amount of air coming out of the diffuser. In most cases, this error is negligible and is less than the accuracy of the instrument. For proportional balancing, this error need not be taken into account because all similar diffusers have about the same amount of back pressure. To determine whether back pressure is significant, a velocity traverse can be made in the duct ahead of the diffuser with and without the hood in place. The difference in average velocity of the traverse indicates the degree of back-pressure compensation required on similar diffusers in the system. For example, if the average velocity is 4.06 m/s (800 fpm) with the hood in place and 4.17 m/s (820 fpm) without the hood, the indicated flow reading can be multiplied by 1.025 on similar diffusers in the system (820/800 = 1.025). As an alternative, the designer of the air-handling system can predict the head-induced airflow reduction by using a curve supplied by the hood manufacturer. This curve indicates the pressure drop through the hood for different flow rates.

E9. Turbine Flowmeters. Turbine flowmeters consist of three basic components: the body, the rotor, and the output device. The flow enters the meter and is directed to the annular passage formed by the inlet cone and the interior wall of the body. The air enters the rotor and, due to the angle of the blades, imparts a force to rotate the rotor. The speed of the rotor is directly proportional to the flow rate. Blade rotation is thus a measure of velocity and is detected by non-contacting external magnetic, photo-chopper, or other proximity detectors. The rotational speed of the rotor is a function of the passageway size and the rotor design. It is also dependent upon internal friction, fluid drags, and fluid density. The relationship between airflow velocity and rotor speed is linear over a wide flow range of up to 100:1. Low flow rate performance is affected by velocity profile, tip clearance, friction across the blades, bearing fiction, and other retarding torques. Since the turbine meter indicates actual volumetric flow, the accuracy of the secondary measurement equipment, such as pressure, temperature, or density, is combined to arrive at an estimated overall uncertainty for the measurement of standard volumetric units.